MIT Libraries | DSpace@MIT

MIT Open Access Articles

ASIRI: An Ocean–Atmosphere Initiative for Bay of Bengal

Citation: Wijesekera, Hemantha W. et al. "ASIRI: An Ocean–Atmosphere Initiative for Bay of Bengal." Bulletin of the American Meteorological Society 97, no. 10 (October2016): 1859–1884. © 2016 American Meteorological Society

As Published: http://dx.doi.org/10.1175/BAMS-D-14-00197.1

Publisher: American Meteorological Society

Persistent URL: http://hdl.handle.net/1721.1/108698

Version: Final published version: final published article, as it appeared in a journal, conference proceedings, or other formally published context

Massachusetts Institute of Technology

ASIRI

An Ocean–Atmosphere Initiative for Bay of Bengal

by Hemantha W. Wijesekera, Emily Shroyer, Amit Tandon, M. Ravichandran, Debasis Sengupta, S. U. P. Jinadasa, Harindra J.S. Fernando, Neeraj Agrawal, K. Arulananthan, G. S. Bhat, Mark Baumgartner, Jared Buckley, Luca Centurioni, Patrick Conry, J. Thomas Farrar, Arnold L. Gordon, Verena Hormann, Ewa Jarosz, Tommy G. Jensen, Shaun Johnston, Matthias Lankhorst, Craig M. Lee, Laura S. Leo, Iossif Lozovatsky, Andrew J. Lucas, Jennifer Mackinnon, Amala Mahadevan, Jonathan Nash, Melissa M. Omand, Hieu Pham, Robert Pinkel, Luc Rainville, Sanjiv Ramachandran, Daniel L. Rudnick, Sutanu Sarkar, Uwe Send, Rashmi Sharma, Harper Simmons, Kathleen M. Stafford, Louis St. Laurent, Karan Venayagamoorthy, Ramasamy Venkatesan, William J. Teague, David W. Wang, Amy F. Waterhouse, Robert Weller, and Caitlin B. Whalen

An observation and modeling campaign in the Bay of Bengal is aimed at studying upper-ocean and lower-atmosphere processes and interactions in relation to Indian Ocean monsoons.

The climate of the tropical ocean and atmosphere is set by monsoons, associated with large-amplitude shifts in the intertropical convergence zone induced by the seasonal cycle of solar insolation with differential heating over the land and ocean. Arguably, the most striking and intense monsoon is the Indian Ocean monsoon (IOM), which drastically affects the livelihoods of more than a billion people in Indian Ocean rim nations (Gadgil 2003).

The large-scale pressure gradients that drive the IOM are strongly modified by air–sea interactions, leading to pronounced subseasonal variability, particularly in the Bay of Bengal (BoB; e.g., Schott and McCreary 2001). This region has been the focus of several previous field campaigns aimed at air–sea interaction and monsoon variability (e.g., Bhat et al. 2001; Webster et al. 2002; Rao et al. 2011). For example, the Bay of Bengal Monsoon Experiment (BOBMEX) examined organized convection using data collected during July–August 1999 (Bhat et al. 2001). The Joint Air–Sea Monsoon Interaction

Experiment (JASMINE) addressed intraseasonal and interannual variability of the monsoon in the eastern Indian Ocean spanning 5°S–15°N (Webster et al. 2002). The Indian government research program, continental tropical convergence zone (CTCZ), investigated intraseasonal variability and monsoon break cycles using observations collected in the northern BoB in July–August 2009 (Rao et al. 2011). Collectively, these studies have improved our understanding of ocean–atmosphere processes in this region; however, significant gaps in our understanding remain, particularly in relation to the role of small-scale ocean processes in ocean heat and freshwater fluxes and in air–sea interaction.

Understanding and prediction of the spatiotemporal evolution of the BoB upper-ocean structure and its linkage to the northern Indian Ocean (IO) has been impeded because of uncertainty in the freshwater distribution, set by high rainfall and river runoff. Since shallow, salinity-controlled mixed layers (MLs) have a strong influence on the distribution of upper-ocean

heat content and sea surface temperature (SST), determining the mixing pathways of river runoff and quantifying the upper-ocean freshwater budget are a priority. The importance of freshwater inputs and formation of shallow mixed layers for the monsoon has been previously noted by Shenoi et al. (2002), and Rao and Sivakumar (2003) made a first-order attempt to quantify the sea surface salinity budget on a seasonal basis using historical hydrophysical fields. At the basin scale, circulation and advection of salinity are strongly controlled by wind and remote equatorial forcing [Schott and McCreary (2001), Shankar et al. (2002), Jensen (2001, 2003), Vialard et al. (2009), Durand et al. (2009), Girishkumar et al. (2013), Vinayachandran et al. (2013), Yu et al. (1991), Potemra et al. (1991), and Yu and McPhaden (2011) are a few references out of many]. The monsoon-driven, seasonally reversing currents alternately export low-salinity BoB water into the Arabian Sea (AS) via the East India Coastal Current (EICC) and Winter Monsoon Current (WMC) and import saltier Arabian Sea water into the BoB via the Summer Monsoon Current (SMC; e.g., Murty et al. 1992; Schott et al. 1994; Shetye et al. 1996; McCreary et al. 1996; Schott and McCreary 2001; Jensen 2001, 2003; Durand et al. 2009; Vinayachandran et al. 2013; Mukherjee et al. 2014). Monsoonal forcing also induces energetic mesoscale and submesoscale features, which complicate the regional oceanographic circulation, and, consequently, it is not completely clear how the BoB and Arabian Sea interact with each other and with the Indian Ocean equatorial region in distributing freshwater. Furthermore, the details of how upper-ocean processes regulate the freshwater distribution and influence air–sea interactions are poorly understood.

Improving the predictability of coupled air–sea models requires a more detailed understanding of the space–time variability of the BoB and physical parameterizations that accurately capture relevant submesoscale and small-scale physics. The initiative Air–Sea Interactions in the Northern Indian Ocean (ASIRI) is a direct response to this need. ASIRI addresses regional-scale air–sea interactions, atmospheric boundary layer structure, and ocean circulation in the BoB using both the observations and numerical models (Lucas et al. 2014). ASIRI combines the first concurrent field observations of small- to regional-scale ocean observations spanning the entire BoB over multiple seasons with high-resolution air–sea coupled modeling.

Facilitated by the Office of Naval Research, ASIRI melds the resources of partner country initiatives, which include the Ocean Mixing and Monsoons (OMM) program of the Monsoon Mission of India, the Coastal Currents Observations Program (CCOP) of the National Aquatic Resources Research and Development Agency (NARA) of Sri Lanka, the Effects of Bay of Bengal Freshwater Flux on Indian Ocean Monsoon (EBOB) program of the U.S. Naval Research Laboratory, and Remote Sensing of Atmospheric Waves and Instabilities (RAWI), a joint initiative between the United States, NARA, Seychelles, Singapore, and the U.S. Army Research Laboratory (ARL). Here we describe the initial findings of the ASIRI project, focusing on ocean observations. In addition, marine mammal observations were conducted (described in the sidebar "Marine Mammal Observations").

SCIENTIFIC RATIONALE AND OBJEC-TIVES.
ASIRI's primary aim is to understand the dominant mesoscale and submesoscale processes that determine the freshwater distribution, including transport and mixing terms, and to determine the influence of upper-ocean structure on air–sea

AFFILIATIONS: Wijesekera, Jarosz, Jensen, Teague, and Wang—Naval Research Laboratory, Stennis Space Center, Mississippi; Shroyer and Nash—Oregon State University, Corvallis, Oregon; Tandon, Ramachandran, and Buckley—University of Massachusetts Dartmouth, Dartmouth, Massachusetts; Ravichandran—Indian National Centre for Ocean Information Systems, Hyderabad, India; Bhat and Sengupta—Indian Institute of Science, Bangalore, India; Jinadasa and Arulananthan—National Aquatic Resources Research and Development Agency, Colombo, Sri Lanka; Fernando, Lozovatsky, Conry, and Leo—University of Notre Dame, Notre Dame, Indiana; Agrawal and Sharma—Space Applications Centre, Ahmedabad, India; Baumgartner, Farrar, Mahadevan, St. Laurant, and Weller—Woods Hole Oceanographic Institution, Woods Hole, Massachusetts; Centurioni, Hormann, Johnston, Lankhorst, Lucas, Mackinnon, Pham, Pinkel, Rudnick, Sarkar, Send, Waterhouse, and Whalen—Scripps Institution of Oceanography, La Jolla, California; Lee, Rainville, and Stafford—Applied Physics Laboratory, University of Washington, Seattle, Washington; Gordon—Lamont–Doherty Earth Observatory of Columbia University, Palisades, New York; Omand—University of Rhode Island, Narragansett, Rhode Island; Simmons—University of Alaska Fairbanks, Fairbanks, Alaska; Venayagamoorthy—Colorado State University, Ft. Collins, Colorado; Venkatesan—National Institute of Ocean Technology, Chennai, India

CORRESPONDING AUTHOR: Hemantha Wijesekera, Naval Research Laboratory, Stennis Space Center, MS 39529
E-mail: hemantha.wijesekera@nrlssc.navy.mil

interactions in the Bay of Bengal. The specific objectives of ASIRI are to

- observe atmospheric (moisture, temperature, winds, and surface fluxes) and upper-ocean (currents, temperature, salinity, and turbulent diffusivity) properties throughout the BoB from diurnal to seasonal time scales;
- examine the role of the freshwater distribution on SST, mixed layer depth, barrier layer strength and evolution, stratification, and currents;
- characterize the coastal boundary current, tides, internal waves, and mixing around Sri Lanka in relation to interbasin exchanges;
- improve quantitative understanding of seasonally varying mesoscale phenomena (e.g., the Sri Lanka dome and transbasin eddies) and their influence on air–sea interaction;

- observe and understand subseasonal to seasonal variability of the atmospheric boundary layer (ABL) and ocean MLs and their feedbacks with basin-scale propagation of the intraseasonal oscillation (ISO; Sengupta et al. 2001) and Madden–Julian oscillation (MJO; Madden and Julian 1971) events.

FIELD PROGRAM. The ASIRI initiative includes multiyear field surveys (Tables 1 and 2) integrated with atmosphere–ocean coupled model simulations (Table 3). Ocean field observations span the microscale, $O(1)$ cm to regional scale $O(1,000)$ km, by including short intensive shipboard campaigns with multiyear mooring and drifter deployments (Fig. 1). ASIRI also integrates remote sensing products, air–sea atmospheric flux measurements, and ABL observations.

TABLE 1. **ASIRI lead principal investigators (PIs) and institutions concerned with ocean observations in the BoB. (Full institution names can be found in the affiliations.) Observations included temperature** T**, salinity** S**, pressure** P**, currents, SST, SSS, SSH, microstructure, AOP, IOP, fast repetition rate fluorometer (FRRF), and color. Policies of data sharing are described in a sidebar.**

Institutions (lead PIs)	Instruments/platforms	Observations
UW (Lee), NARA	Seagliders	T, S, P, profiles
SIO (Rudnick)	Spray gliders, profiling floats	T, S, P, profiles
SIO (Centurioni), NARA	SVP drifters	Surface currents
IIS (Sengupta), INCOIS (Ravichandran), NIOT (Venkatesan)	Drifters	Surface currents
SIO (Send), NARA	PIES	SSH, currents
NARA (Jinadasa), ND, NRL	ADCP, CTD, strings	Currents, T, S, P
SIO (Mackinnon, OSU (Shroyer)	CTD, UCTD, ADCP	T, S, P, currents
IIS (Sengupta), INCOIS (Ravichandran), NIOT (Venkatesan)	CTD, UCTD, XBT, expendable CTD (XCTD), ADCP	T, S, P, currents
OSU (Nash)	Towed chain	T, S, P, profiles
SIO (Lucas)	Wirewalker	Microstructure
NRL (Wijesekera)	ScanFish	T, S, P, profiles
WHOI (St. Laurent)	Slocum glider	Microstructure
IIS (Sengupta)	Microprofiler	Microstructure
ND (Lozovatsky)	VMP	Microstructure
OSU (Moum, Shroyer, Nash)	Chi pods	Microstructure
NARA (Jinadasa), ND (Lozovatsky)	VMP	Microstructure
UW (D'Asaro)	Lagrangian floats	Mixed layer T, S, P
WHOI (Mahadevan)	Fluorometer, hyperspectral radiometer	AOP, IOP, FRRF
IIS (Sengupta), INCOIS (Ravichandran), NIOT (Venkatesan)	Fluorometer, hyperspectral, radiometer	AOP, IOP, FRRF
SAC (Sharma, Agarwal)	Satellite	SST, SSH, SSS, color
NRL (Wijesekera)	Subsurface moorings	T, S, P, currents
WHOI (Weller, Farrar)	Surface mooring	T, S, P, currents
LDEO (Gordon)	Hydrographic data	T, S, P, currents

Ocean measurements. Long-term time series are being collected through multiyear mooring deployments, which include a six-element water column subsurface array distributed between 5° and 8°N and 85.5° and 88.5°E in the southern BoB and a solo deployment near 18°N, 89°E in the northern BoB (Figs. 1, 2a,b). The NRL-led southern array was deployed in December 2013 and was successfully recovered in August 2015. These subsurface moorings provide currents in the upper 600 m from acoustic Doppler currents profilers (ADCPs), supplemented by hydrographic data and turbulent dissipation rates

at selected depths using Sea-Bird MicroCats and Chi pods (Moum and Nash 2009), respectively. The shallowest measured depth of currents is 8 m below the surface. The Woods Hole Oceanographic Institution (WHOI)–OMM 18°N mooring deployment spans December 2014–January 2016 and provides concurrent measurements of surface meteorology; air–sea fluxes of heat, freshwater, and momentum; and upper-ocean temperature, salinity, velocity, and turbulent mixing. Three nearby Research Moored Array for African–Asian–Australian Monsoon Analysis and Prediction (RAMA; McPhaden et al. 2009) moorings maintained by the National Oceanic and Atmospheric Administration (NOAA) and five moorings maintained by the National Institute of Ocean Technology (Chennai, India) augment the specialized instrument deployments (Fig. 1).

The Lagrangian Drifter Laboratory at the Scripps Institution of Oceanography (SIO) partnered with NARA to deploy three Surface Velocity Program (SVP) drifters drogued at 15-m depth (Niiler 2001) every month off Sri Lanka between May 2013 and September 2015, primarily using the research vessel (R/V) *Samudrika*. A total of 64 satellite-tracked SVP drifters were deployed between 2013 and 2014 (Figs. 1, 3a). A thermistor on all SVP drifters measured the SST every 15 min, with the data being transmitted on a roughly 1–2-h basis. In addition to these regular deployments, during the 2015 field campaign a one-time deployment of 36 salinity SVP drifters was used
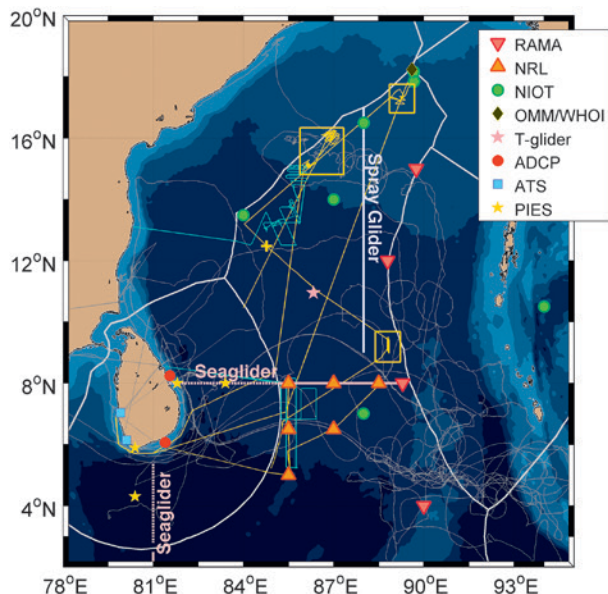

FIG. 1. Map illustrating BoB multiyear observational program. The color image represents the bathymetry and the white lines are the exclusive economic zones (EEZs). Thin yellow and thin blue lines are the R/V *Roger Revelle* tracks for legs 1, 2, and 3 in Nov–Dec 2013 and in Jun–Jul 2014. Thick white lines and purple line denote Seaglider and Spray Glider tracks, respectively. The yellow rectangle near 19°N, 89°E is the region where a process study was conducted in Aug–Sep 2014 from *Sagar Nidhi*. The black diamond, orange triangles, green bullets, and red triangles denote locations of WHOI–OMM, NRL, NIOT, and RAMA moorings, respectively. Two red circles are locations of ADCP moorings. PIESs are marked by yellow stars. The weather stations and atmospheric measurement towers in Sri Lanka are marked by blue squares. The purple star denotes turbulent glider observations. Thin gray lines are surface drifter tracks.

to map the sea surface salinity (SSS) and SST distributions and variability in the northern BoB at higher temporal and spatial resolution.

Partnered with NARA scientists, volume transports of boundary currents around Sri Lanka are being measured using pressure sensor–equipped inverted echo sounders (PIESs), which record seafloor pressure and acoustic travel time vertically through the entire water column. Two PIESs were deployed on the path of the EICC along 8°N (Fig. 1) during November 2014 from the R/V *Samudrika*, and another two PIESs were deployed along the 80.4°E off southern Sri Lanka in December 2015 for a duration of deployment of up to 4 years with data subsets transmitted through acoustic modems; all data will be retrieved after recovery of the instruments. The data can be projected onto vertical modes of variability in the boundary current and together with satellite altimetry will constrain the boundary current variability with improved understanding of the vertical structure. The first year of PIESs data was retrieved via acoustic telemetry from the 8°N section in November 2015.

Table 3. ASIRI lead PIs and institutions focused on BoB modeling.	
Institutions (lead PIs)	**Model**
NRL (Jensen)	Ocean–atmosphere coupled
UA (Simmons)	Regional scale
WHOI (Mahadevan)	Bio-optical
UMassD (Tandon)	Submesoscale
SIO and UCSD (Sarkar)	Small scale
CSU (Venayagamoorthy)	Small scale

On the basin scale, six University of Washington Seagliders, deployed in collaboration with NARA from the R/V *Samudrika* and chartered vessels, have sampled large-scale gradients and mesoscale variability over the upper 1,000 m. The glider measurements focus on the annual cycle of the lateral and vertical structure of water mass variability and mixing (Fig. 4). Two Seaglider survey lines have been maintained since 2013 in the southern BoB; one along 8°N between east of Sri Lanka and 90°E, and the other along 81°E between south of Sri Lanka and 2°N (Figs. 1, 4). Two
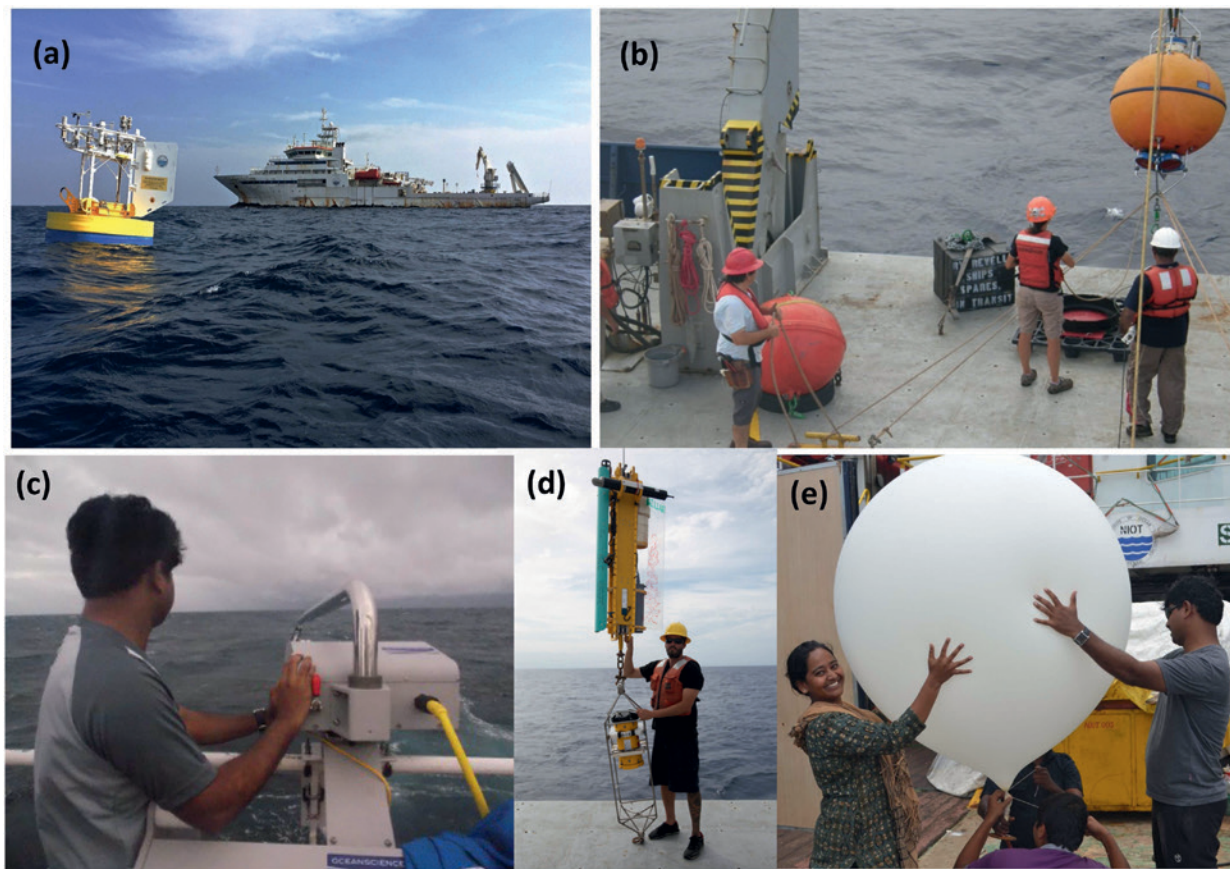

Fɪɢ. 2. (a) WHOI–OMM surface mooring from the *Sagar Nidhi*, (b) deployment of NRL subsurface moorings from the *Roger Revelle*, (c) deploying UCTD, (d) deploying a WW profiling package with multiple sensors, and (e) deploying radiosonde from the *Sagar Nidhi*.
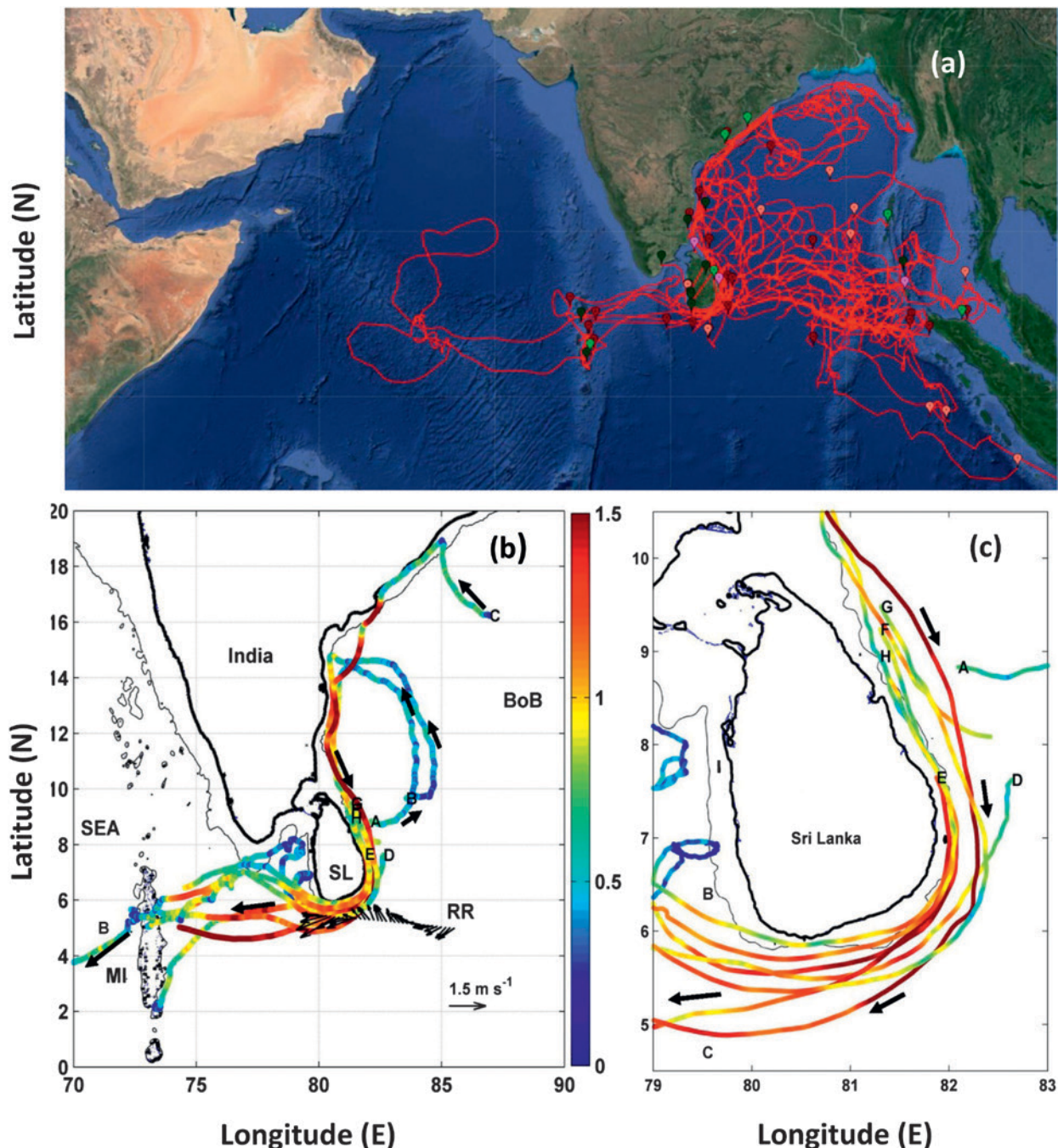
Fig. 3. (a) Tracks of 64 SVP drifters deployed during 2013/14. (b) Tracks of eight drifters deployed east of Sri Lanka and in southern BoB between 24 Oct and 23 Dec 2013 showing the EICC. (c) Drifter tracks (A–H) and speeds (color shading) in m s⁻¹. The arrows indicate velocity vectors at 21.5-m depth along the *Roger Revelle* track on 23–24 Dec 2013 from 150-kHz ADCP. (right) Enlarged view of drifter tracks and speeds around Sri Lanka.

Spray underwater gliders have been deployed to run a north–south line along 88°E between 9° and 17°N (Fig. 1). Three additional Sounding Oceanographic Lagrangian Observer-II (SOLO-II) profiling floats were deployed in the north-central BoB to supplement the international Argo campaign and to provide a complimentary perspective to long-range glider transits.

Multiple shipboard campaigns provide large-scale rapid surveys, intensive feature tracking, and small-scale process studies using the R/V *Roger Revelle* and R/V *Sagar Nidhi* (Fig. 1; Table 1). Measurements were expanded to resolve near-surface properties through inclusion of two additional high-frequency ADCPs and a bow-mounted *T–S* chain. Rapid ship-based
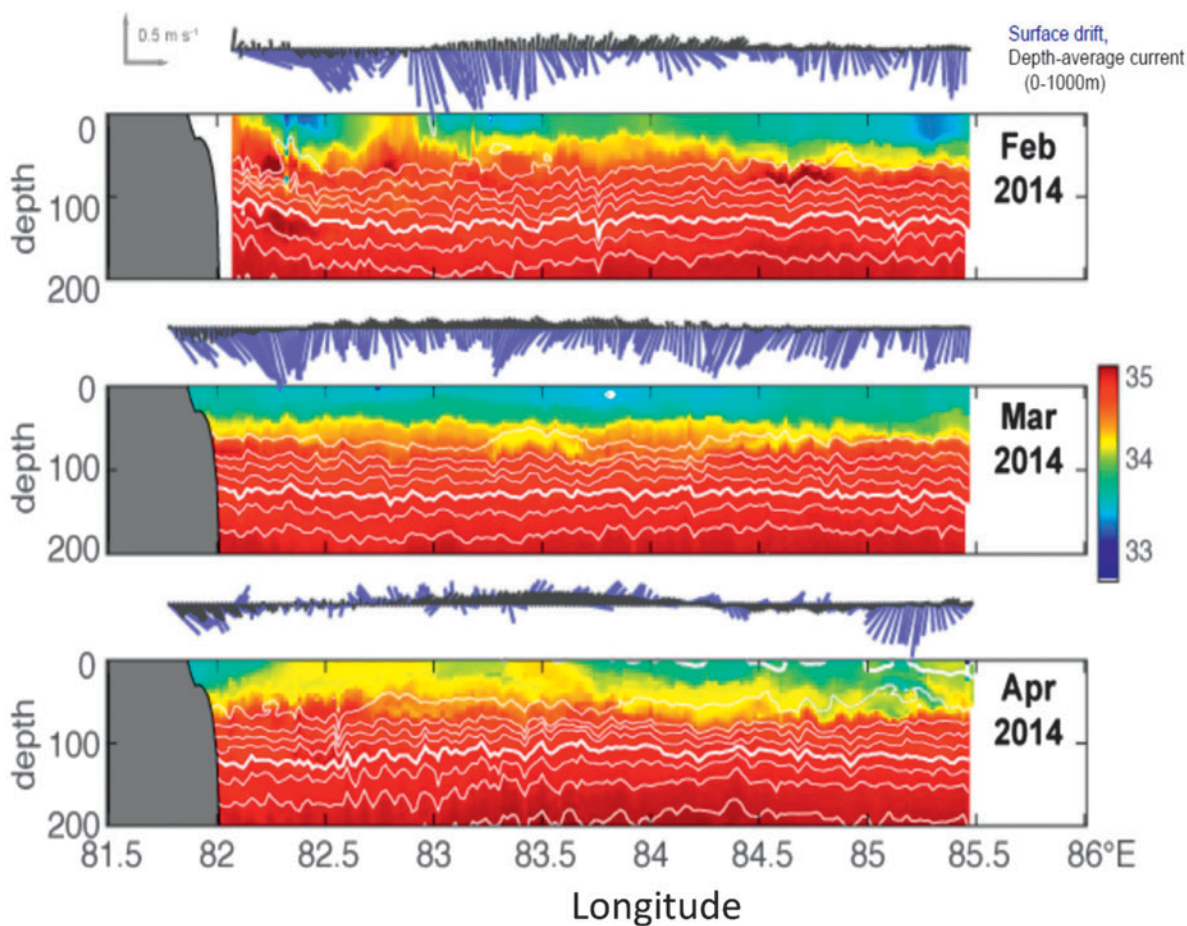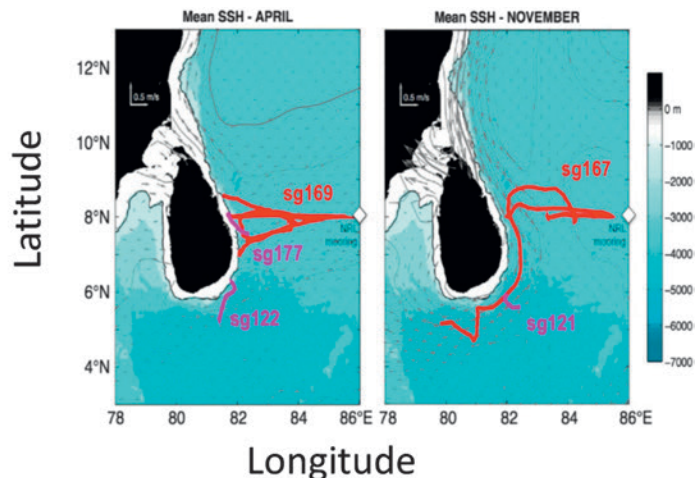
Fig. 4. (top left) Deploying Seagliders from R/V *Samudrika*. (top right) Glider tracks off the east coast of Sri Lanka. (bottom) Depth–longitude sections of salinity along 8°N and depth-averaged currents in Feb, Mar, and Apr 2014.

profiling was accomplished using multiple platforms, including Oceanscience's underway conductivity–temperature–depth profiler (UCTD; Fig. 2c); a ScanFish, towed, undulating profiler; and the SIO's FastCTD system. Turbulent mixing rates, inherent and apparent optical properties (IOP/AOP), nutrients, and CTDs

were collected from the ship-based vertical profilers (Table 1). Coastal and western boundary surveys around Sri Lanka were carried out using the R/V *Samudrika*, gliders, drifters, and PIES.

Short-term autonomous assets, including mixed layer floats, upper-ocean profiling floats, near-surface spar

South of Sri Lanka
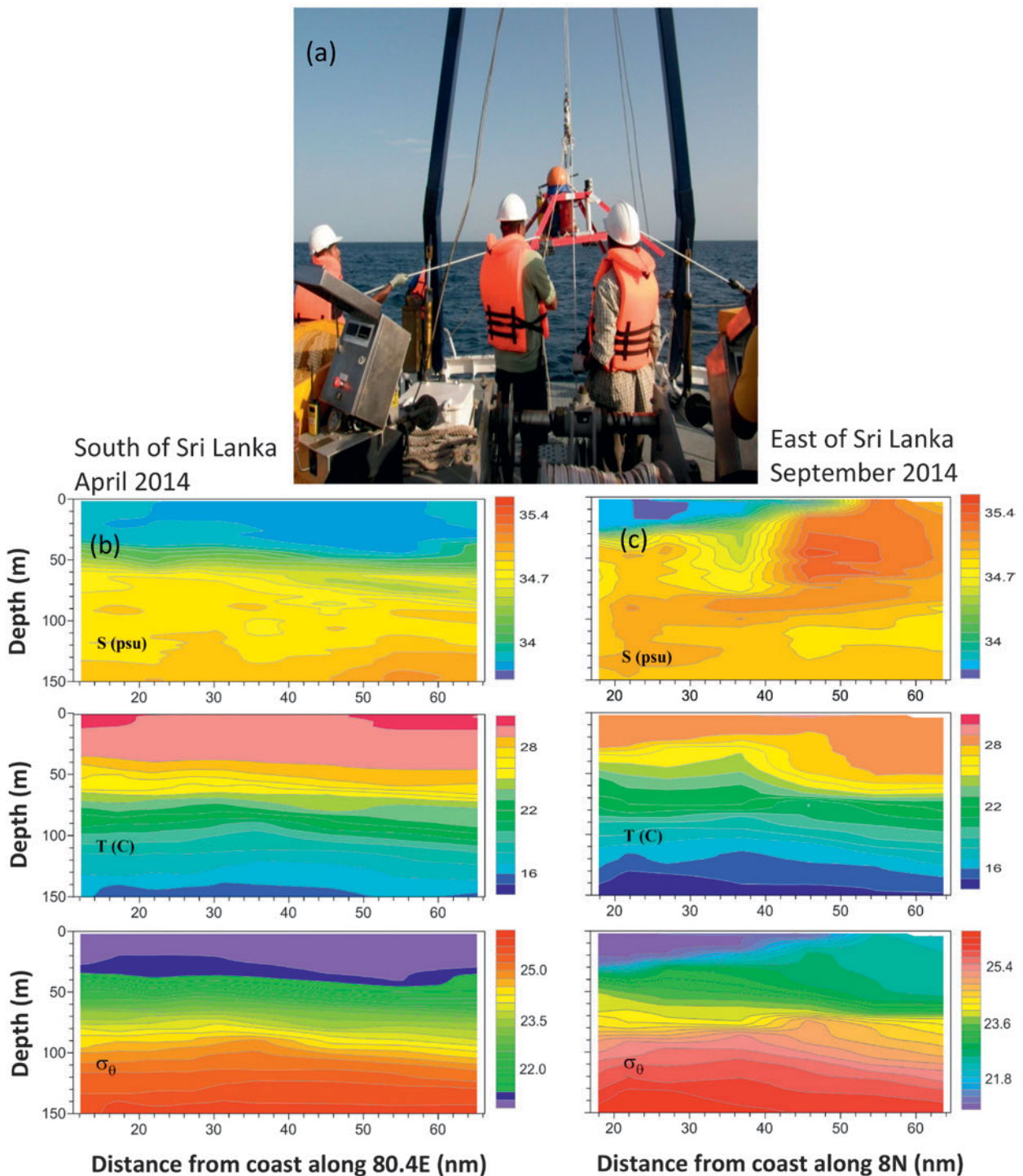April 2014

East of Sri Lanka
September 2014

FIG. 5. (a) NARA scientists deploying a bottom-mounted ADCP pod near 8°N off the east coast of Sri Lanka in Jul 2014 from the R/V *Samudrika*. (b) The southern (Apr 2014) and (c) the eastern (Sep 2014) sections of (top) salinity, (middle) temperature, and (bottom) density.

buoys, profiling wirewalkers (WWs), and microstructure gliders, provided an uncontaminated view of the near-surface and shallow mixed layer characteristics of the BoB. For example, drifting wirewalker (Fig. 2d) arrays (3–4 units) formed the reference for high-resolution

ship sampling during the 2013 and 2014 cruises on the R/V *Roger Revelle*. Wirewalkers use energy from the surface wavefield to drive a vehicle vertically along a wire (Pinkel et al. 2011; Rainville and Pinkel 2001). The resulting rapid profiling down to 150 (2013) and
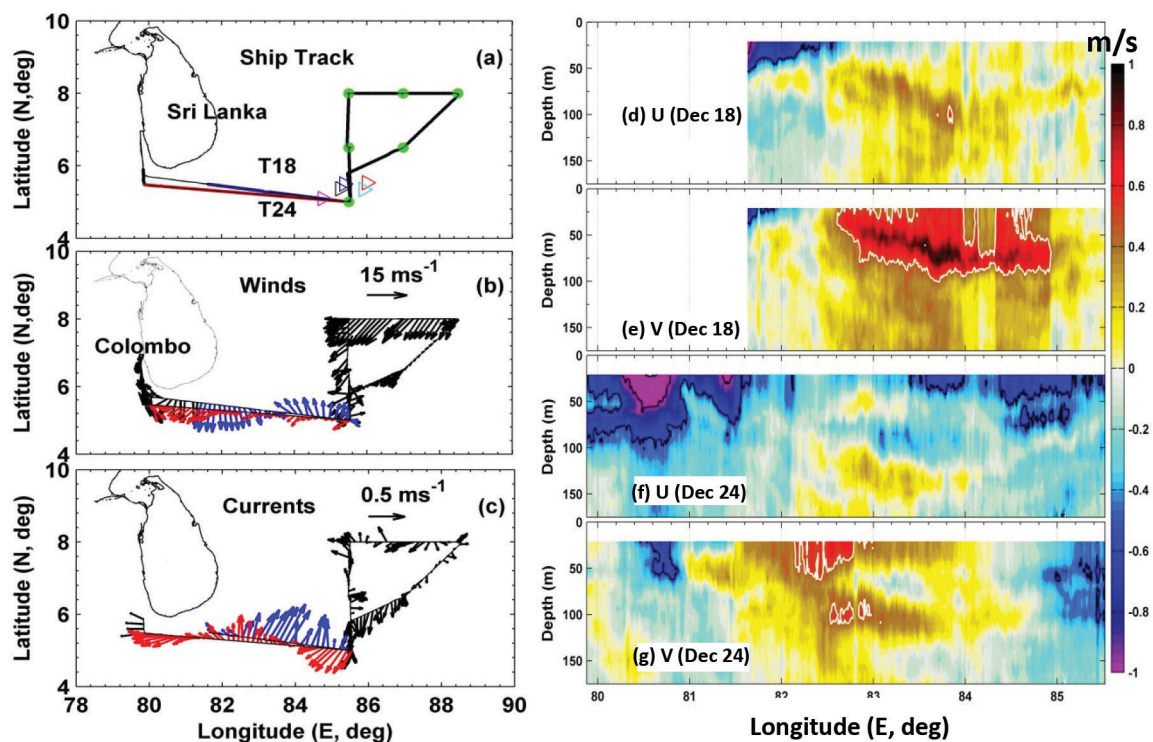
Fig. 6. Winter monsoon currents in the southern BoB. (a) R/V *Roger Revelle* tracks during leg 3. T18 is the ship transect on 18 Dec 2013, and T24 is the ship transect on 23–24 Dec. The green dots represent the mooring and CTD locations. (b) Wind vectors based on hourly averages along the ship track. Blue and red arrows denote winds along T18 and T24, respectively. (c) Upper 175-m depth-averaged ADCP current vectors along the ship track. Velocity along (d),(e) T18 and (f),(g) T24. Sections of (d),(f) zonal velocity *U* and (e),(g) meridional velocity *V*. Velocity contours of −1 and −0.5 m s⁻¹ are marked by black lines, and contours of +0.5 m s⁻¹ are marked by white lines.

100 m (2014) provided one profile every 15 and 10 min, respectively. Wirewalker sensors included CTD, current, chlorophyll fluorescence, colored dissolved organic matter (CDOM), optical backscatter, dissolved oxygen, hyperspectral irradiance, and temperature microstructure.

Satellite observations. Satellite products are used to examine BoB submesoscale to regional scale, and diurnal to seasonal variability include merged products of sea surface height anomaly (SSHA; www.aviso .altimetry.fr/en/data.html; e.g., Kurien et al. 2010; Cheng et al. 2013), SST, and outgoing longwave radiation (OLR) from geostationary platforms, high-resolution (1 km) Group for High-Resolution Sea Surface Temperature (GHRSST) and NOAA Advanced Very High Resolution Radiometer (AVHRR), Sea-viewing Wide Field-of-view Sensor (SeaWiFS), Ocean Color Monitor (OCM), and Moderate Resolution Imaging Spectroradiometer (MODIS) products. Synthetic aperture radar (SAR) missions, *Radar Imaging Satellite* (*RISAT*), *Radarsat-2* (www.asc-csa.gc.ca/eng /satellites/radarsat2/), and *TerraSAR-X* are being used

to examine finescale fluctuations and internal waves. The SSS products from Aquarius (launched in 2011 and ended on 8 June 2015) and Soil Moisture Ocean Salinity (SMOS; e.g., Lagerloef et al. 2010) will be used to understand the seasonal variability of salinity at large scales.

ABL measurements. ASIRI–RAWI is targeting atmospheric phenomena with oscillations on the order of 30–90 days (e.g., MJO) and shorter, including quasi-biweekly oscillations (QBO) as well as synoptic and mesoscale phenomena down to turbulence in the surface layer. To this end, a suite of meteorological instruments was deployed from February through March 2015 in the Seychelles (4.68°S, 55.53°E), Sri Lanka (6.98°N, 79.87°E), and Singapore (1.3°N, 103.77°E) to capture the propagation of such disturbances through the BoB (http://ceees.nd.edu /research-facilities/projects/asiri-rawi). Collectively, various sites acquired vertical profiles of temperature, humidity, wind speed, wind direction, vertical velocity, cloud cover, precipitation, and radiation as well as
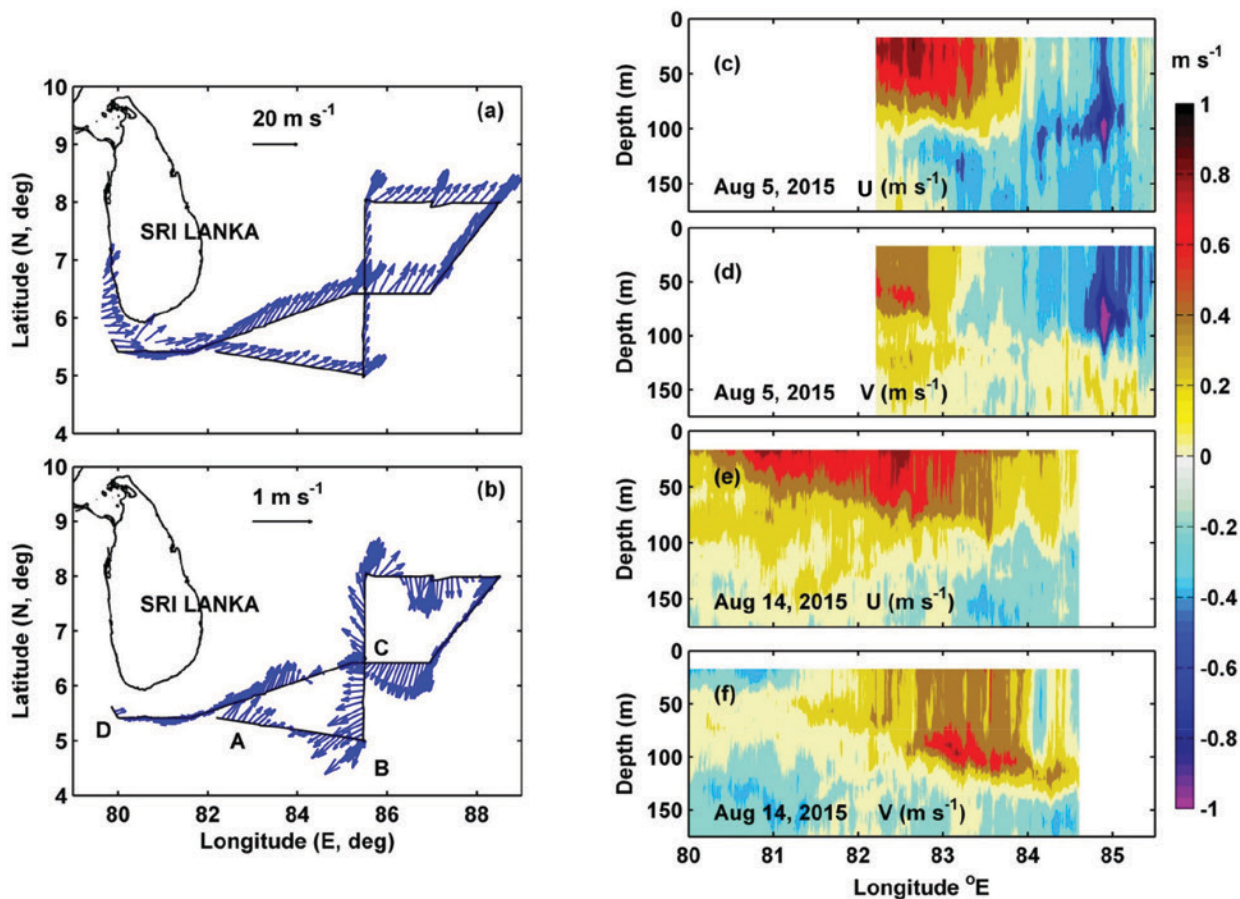
FIG. 7. Summer monsoon currents in the southern BoB. (a) Wind vectors along the R/V *Roger Revelle* tracks during the mooring recovery in Aug 2015. (b) Upper 175-m depth-averaged ADCP current vectors along the ship track. Sections of (c) zonal velocity *U* and (d) meridional velocity *V* along the outbound track and (e) *U* and (f) *V* along the inbound track.

momentum, heat, and moisture flux measurements using flux towers. Coastal Sri Lankan and Seychelles sites included a microwave radiometer, Doppler wind lidar, ceilometer, and 2–3 daily radiosondings [released at World Meteorological Organization (WMO) stations 43466 and 63985, respectively]. The Singapore site featured lidar and two daily soundings

(at WMO 48698). All sites had a flux tower (10–13 m) with 3D sonic anemometers at multiple levels; two sites also included infrared gas analyzers and net radiometers for moisture fluxes and solar radiation measurements, respectively. Additional radiosonde measurements were collected away from land using the R/V *Sagar Nidhi* (Fig. 2e). Details of atmospheric

DATA SHARING

The data collected in international waters of the Bay of Bengal as part of ASIRI–EBOB and ASIRI–OMM will be available to the research community worldwide. The data collected by ONR and NRL investigators are embargoed for a period of 3 years to allow quality assurance (QA)/quality control (QC) of data and completion of publications. Outputs of model simulations conducted

by the NRL will also be available at the U.S. Navy Department of Defense (DoD) Supercomputing Resource Center. The above data sharing policies do not apply to those data collected by the international partners, who will follow their internal protocols and ASIRI–EBOB and ASIRI–OMM agreements. Restrictions apply to data collected in EEZs or inland of partner

countries, who have granted access on special terms. The sharing of water column observations within Sri Lanka territorial waters requires written permission from the National Aquatic Resources Research and Development Agency, Sri Lanka. Hosting of the bulk of data on a central database is being considered. For inquiries about data sharing contact the first author.

observations, instrumentation, and contributing institutions are given in Table 2.

OBSERVATIONS AND PRELIMINARY RESULTS.

A total of six cruises were successfully conducted in international waters of the BoB using the R/V *Roger Revelle* in collaboration with the R/V *Sargar Nidhi*. Five *Roger Revelle* cruises were carried out from Colombo, Sri Lanka, in November–December 2013, July–August 2014, and August 2015; two *Revelle* cruises took place out of Chennai, India, in June 2014 and August–September 2015. Three *Sagar Nidhi* cruises were conducted in November–December 2013, August–September 2014, and August–September 2015. Since January 2013, coastal and boundary current observations around Sri Lanka have been carried out by the R/V *Samudrika*. A few preliminary results from the integrated observational efforts are summarized below.

Coastal transports and boundary currents around Sri Lanka. Circulation and hydrographic structure over the Sri Lankan shelf, slope, and deep ocean (Fig. 1) were examined through collaborations between NARA and U.S. partners (Fig. 5a). Many of these observations are the first of their kind in this region. Sea surface height anomaly [Archiving, Validation, and Interpretation of Satellite Oceanographic Data (AVISO)] indicates that the boundary current across the section east of Sri Lanka is dominated by semiannual variability, while annual variability dominates the section south of Sri Lanka. The 2014 PIES observations confirm a semiannual variability in transport to the east of Sri Lanka. In situ observations include CTD and microstructure measurements that were collected along two offshore transect lines: a zonal transect along 8°N and a meridional transect along 80.4°E (Figs. 5b,c). These hydrographic observations illustrate the differences in stratification around Sri Lanka during April and September. In late April, the mixed layer depth (MLD) along
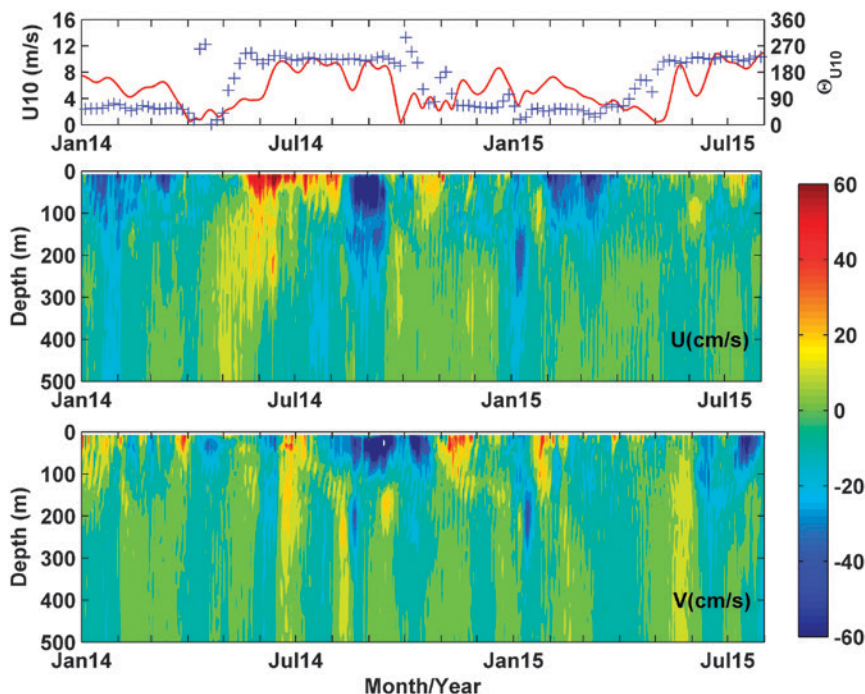

FIG. 8. (top) Time series of daily averaged wind speed (red) and direction (blue +) from the RAMA buoy at 12°N, 90°E, and time–depth section of (middle) 36-h low-passed filtered zonal velocity and (bottom) meridional velocity from the NRL mooring at 6.5°N, 87°E (Fig. 1).

80.4°E varied between 20 and 30 m. In September, the thermohaline structure off the east coast of Sri Lanka indicated that there was a sharp front over about 10 nautical miles (n mi; 1 n mi = 1.852 km) at ~40 n mi from the coast. The onshore side of the front contained a 10–20-m-thick layer with low-salinity (<33.8 psu) and high-temperature (>28.5°C) water, while its offshore side had a deeper mixed layer with a subsurface (~50 m) salinity maxima. Seaglider hydrographic sections along 8°N indicate rising isohalines near the Sri Lankan coast in February 2014 and a more patchy salinity field in April 2014. In February and March, depth-averaged flows were typically near 0.5 m s^{-1}; the currents were weaker and more variable in April (Fig. 4).

Regular Lagrangian drifter deployments in the coastal waters of Sri Lanka provide information about the lateral structure, flow patterns, and speeds of the boundary current east of southern India and around Sri Lanka (Fig. 3a). During November–December 2013, the EICC (Figs. 3b,c) was confined to a narrow boundary current southeast of India and east of Sri Lanka prior to developing into an approximately 200-km-wide current as it turned to the west, south of Sri Lanka. Shipboard ADCP sections from December 2013 show the subsurface structure in the vicinity of the EICC (Fig. 6). To the east of the EICC,

The 2-km-resolution ocean compo-nent of COAMPS, the Navy Coastal Ocean Model (NCOM; Martin 2000), includes tides and interacts with a 6-km resolution modeled atmosphere and a 13-km resolution Simulating Waves Nearshore (SWAN) spectral wave model (Booij et al. 1999). These coupled models exchange fluxes every 6 min. This regional coupled model setup has been validated for several regions around the world (Allard et al. 2012). For the BoB, the regional-scale atmospheric and oceanic states are also in good agreement with observa-tions, which is to be expected since the model assimilates data and uses bound-ary conditions from the Navy Global Environmental Model and the global Hybrid Coordinate Ocean Model.

COAMPS fields have been compared to both ocean currents and tempera-ture fields near the equator (Jensen et al. 2015) and shipboard meteorologi-cal observations (Chen et al. 2015).

The simulated near-surface winds, ocean currents, and salinity during the northeast monsoon are shown for December 2013, when the western equatorial Indian Ocean was experienc-ing westerly winds of an MJO event (Fig. SB1). Spatially varying surface wind fields include the intensification of winds between the gap of India and Sri Lanka and a shadow zone southwest of Sri Lanka. A 24-h forecast of salinity at 60 m on 24 December 2013 shows the advection of low-salinity water along the Sri Lanka east coast and the offshore subsurface intrusion of high-

salinity Arabian Sea water, qualitatively similar to the observed fields (Fig. 6). Zonal depth sections of observed and modeled currents along 5.25°N on 23 December 2013 show that the model captures the basic features of the flow, although the strength and locations of currents vary from the observations (Fig. SB2).

Submesoscale processes modeling. The ASIRI submesoscale modeling uses high-resolution process study models capable of resolving O(1–10) km lateral density gradients and instabilities, with finer-scale, large-eddy simulations (LESs) focusing on vertical and lateral mixing at open-ocean bores and bound-ary layer mixing in the presence of bar-rier layers. Previous observational and
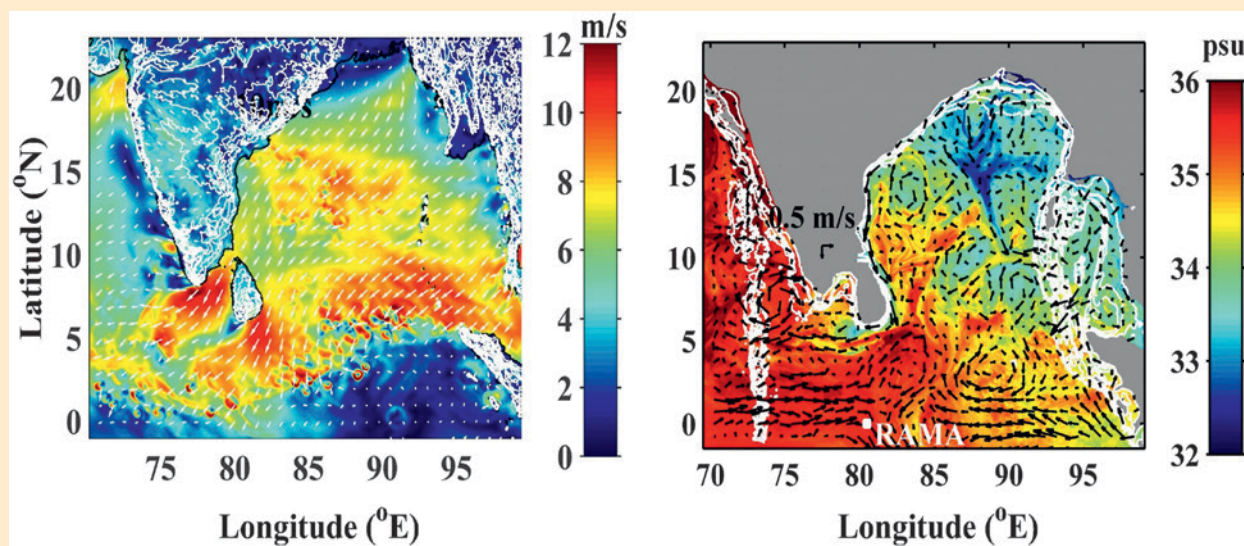

FIG. SB1. (left) Longitude–latitude plot of 10-m wind speed and wind vectors from the 6-km resolution COAMPS nest at 0600 UTC 22 Dec 2013. (right) A 24-h forecast of salinity and current vectors at 60 m from COAMPS on 24 Dec 2013.

a north-northeastward, ~300-km-wide, subsurface flow was observed with speeds >0.5 m s⁻¹ at depths down to about 100 m and with near-surface maxi-mum velocities >1 m s⁻¹ in its core (Fig. 6). Past obser-vations have shown that high-salinity water intrudes into the bay during the southwest monsoon (e.g., Murty et al. 1992). These data show northward flow carried high-salinity water into the BoB during the northeast monsoon as well. These observations are qualitatively consistent with numerical simulations

described in the sidebar on the modeling program (Wijesekera et al. 2015).

Snapshots of the SMC entering into the BoB from south-southeast of Sri Lanka in August 2015 (Fig. 7) reveal notable differences between zonal and meridional components of the SMC; the me-ridional component has a subsurface maximum of about 0.6 m s⁻¹ near 100-m water depth, while the zonal component has a surface maximum of about 0.8 m s⁻¹. CTD casts taken at mooring sites showed

numerical studies (e.g., Mahadevan et al. 2012; D'Asaro et al. 2011; Mahadevan and Tandon 2006) have demonstrated the crucial role of submesoscale instabilities in restratifying the upper ocean in regions with deep [$O(100)$ m] mixed layers. To explore the potential for submesoscale instabilities in monsoon conditions characterized by shallow [$O(10)$ m] mixed layers, a series of submesoscale-resolving simulations have been conducted using the Process Study Ocean Model (PSOM; Mahadevan and Tandon 2006).

For example, a PSOM simulation (Fig. SB3) was initialized with a south–north density gradient inferred from Argo floats near 18°N during August 2013. The horizontal grid resolution is 1 km, and the vertical grid resolution varies from $O(1)$ m at the top to 20 m at the bottom of the domain. The model is forced with daily winds and hourly heat fluxes for August 2013. The precipitation in the model occurs at a rate of 40 mm h^{-1} for 1.5 h, followed by a gap of 2 days before the next rain event. The forcing is imposed after the mixed layer front goes unstable to ageostrophic baroclinic instabilities (Boccaletti et al. 2007; Fox-Kemper et al. 2008) in 4.8 days (approximately three inertial periods). The rainfall was constrained to a 100-km-wide meridional band, thus enabling the exploration of mechanisms for transport of freshwater in a BoB-like regime. Before the onset of surface forcing, mixed layer instabilities (Boccaletti et al. 2007) generate numerous dipole structures with strongly ageostrophic vorticity filaments characterized by $O(1)$ Rossby numbers (Fig. SB3). The presence of forcing disrupts the dipolelike formation of these features and weakens the vorticity field slightly, though filaments with relative vorticity $\zeta \sim O(f)$ continue to exist at the frontal edges. This simulation shows submesoscale signatures in shallow, stratified layers, with conditions markedly different from the deep $O(100)$ m wintertime mixed layers characterizing earlier observational and numerical studies (Boccaletti et al. 2007).

Turbulence process modeling. A three-dimensional LES model (Pham et al. 2013) has been used to understand barrier layer dynamics with unprecedented resolution: $O(cm)$ vertical and $O(m)$ horizontal. The unusually small vertical entrainment by wind forcing found in the LES is consistent with ASIRI observations. The sharp lateral gradients that are ubiquitous in the observations admit the possibility of three-dimensional instabilities and turbulence (Arobone and Sarkar 2015) during equilibration. These processes are also being studied using LES with $O(m)$ resolution in the horizontal and vertical.
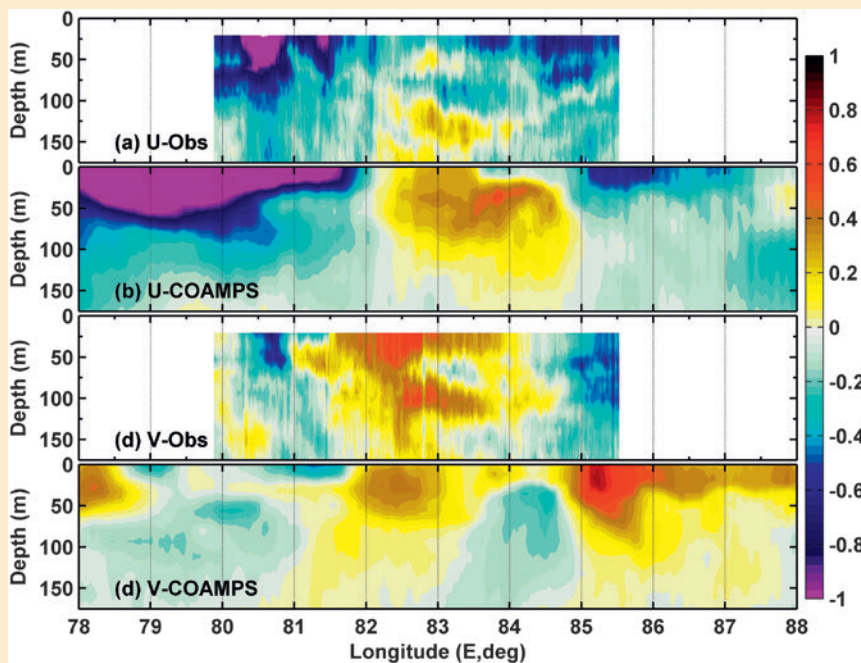

Fɪɢ. SB2. Comparison of (a),(b) zonal and (c),(d) meridional components of velocities from shipboard observations and COAMPS simulations along 5.27°N on 24 Dec 2013. Units are in m s^{-1}.

that a layer of high-salinity water was associated with the northward flow. A similar subsurface water mass structure was discussed by Vinayachandran et al. (2013).

The reversing flow patterns, eddies, and intraseasonal fluctuations are observed in the time–depth sections of velocity from the NRL mooring at 6.5°N, 87°E (Fig. 8). The zonal flow in the upper 200 m was westward during the northeast monsoon (January–March in 2014, 2015) and reversed to eastward during summer monsoon. During summer, the SMC resided between a cyclonic circulation and an anticyclonic eddylike feature to the southeast (e.g., Vinayachandran et al. 1999). Intraseasonal oscillations with periods close to 60 days in the meridional component of velocity are apparent. The mooring observations captured the movement of the SMC/eddy structure, which is also consistent with the AVISO SSH anomalies and drifter tracks (not shown).
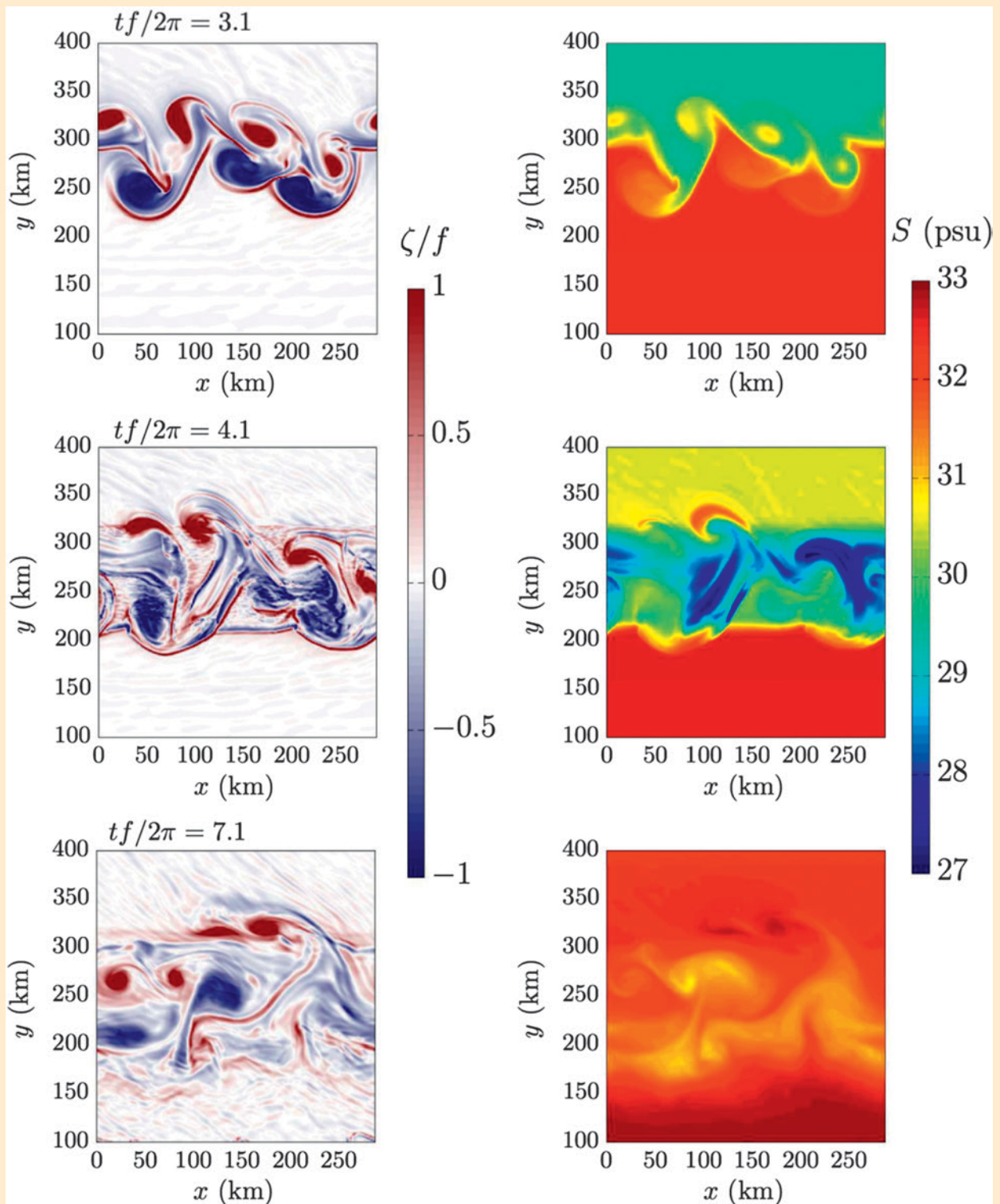
FIG. SB3. Evolution in time *t* of near-surface (*z* = –2.3 m) vorticity and salinity. The winds, heat, and salt fluxes are turned on at *tf*/2π = 3.1. The filaments with O(1) ζ/*f* persist under the influence of surface forcing and rainfall. In spite of the initial freshening due to rainfall, strong mixing results in a significant increase in salinity.
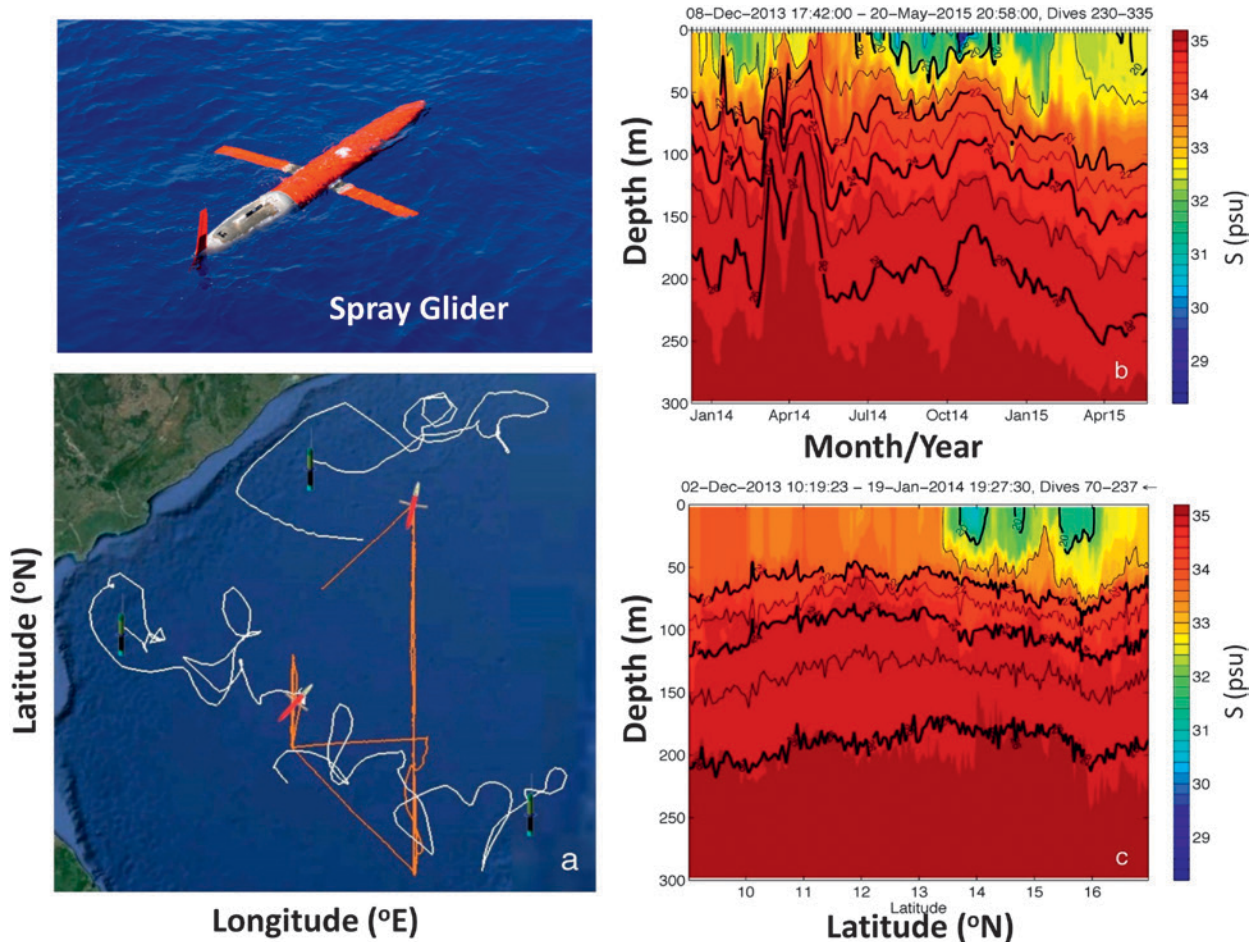
Fig. 9. (top left) Spray underwater glider. (a) Tracks of two Spray gliders and three SOLO-II profiles floats during Nov 2014–May 2015. The float deployments are ongoing, delivering data through the Argo system. Salinity sections (b) from the northern float as a function of time and (c) from the glider as a function of latitude along 88°E. Potential density is indicated by black lines.

Regional and mesoscale variability: Currents, hydrography, and bio-optics. The BoB interior has distinct regional gradients in hydrographic and bio-optic properties (e.g., Murty et al. 1996; Rao et al. 2011; Vinayachandran et al. 2002). Deployments of two Spray underwater gliders and three SOLO-II profiling floats were undertaken with a goal of observing low SSS layers and the underlying regional-scale thermohaline fields (Fig. 9). Over 1,000 profiles, collected to date, show frequent occurrence of low SSS layers, with greater prevalence in the northern BoB. A float deployed in the northern BoB observed an SSS of less than 28.5 psu with a density of less than 1,018 kg m^{-3} in a layer roughly 20 m thick. Salinity drifters have recorded surface salinity as low as 25 in the northern BoB at 200-km distance from the Ganges' delta. This low SSS layer was observed in a sequence of a few profiles separated by 5 days. A glider section in the central BoB showed low SSS layers similar in depth

though with slightly higher salinity. The preliminary analysis suggests that the SSS along Aquarius tracks and the SSS from SOLO-II floats were comparable to one another, suggesting a path toward better quantification of time–space variability in freshwater lenses in future analysis.

Shipboard surveys also provide a means of assessing the spatial variability in low-salinity lenses. For example, the August–September 2014 *Sagar Nidhi* survey in northern BoB (Fig. 2c) measured strongly stratified, shallow, salinity-controlled layers that occasionally outcropped at the surface (Fig. 10b). In this data record, subsurface, large lateral gradients in *T* and *S* and near-surface stratification are enhanced under fronts.

During the November–December 2013 leg of the *Roger Revelle*, the large-scale underway CTD mapping was interspersed with regular CTD rosette stations approximately every 40 n mi for a total of 81 rosette
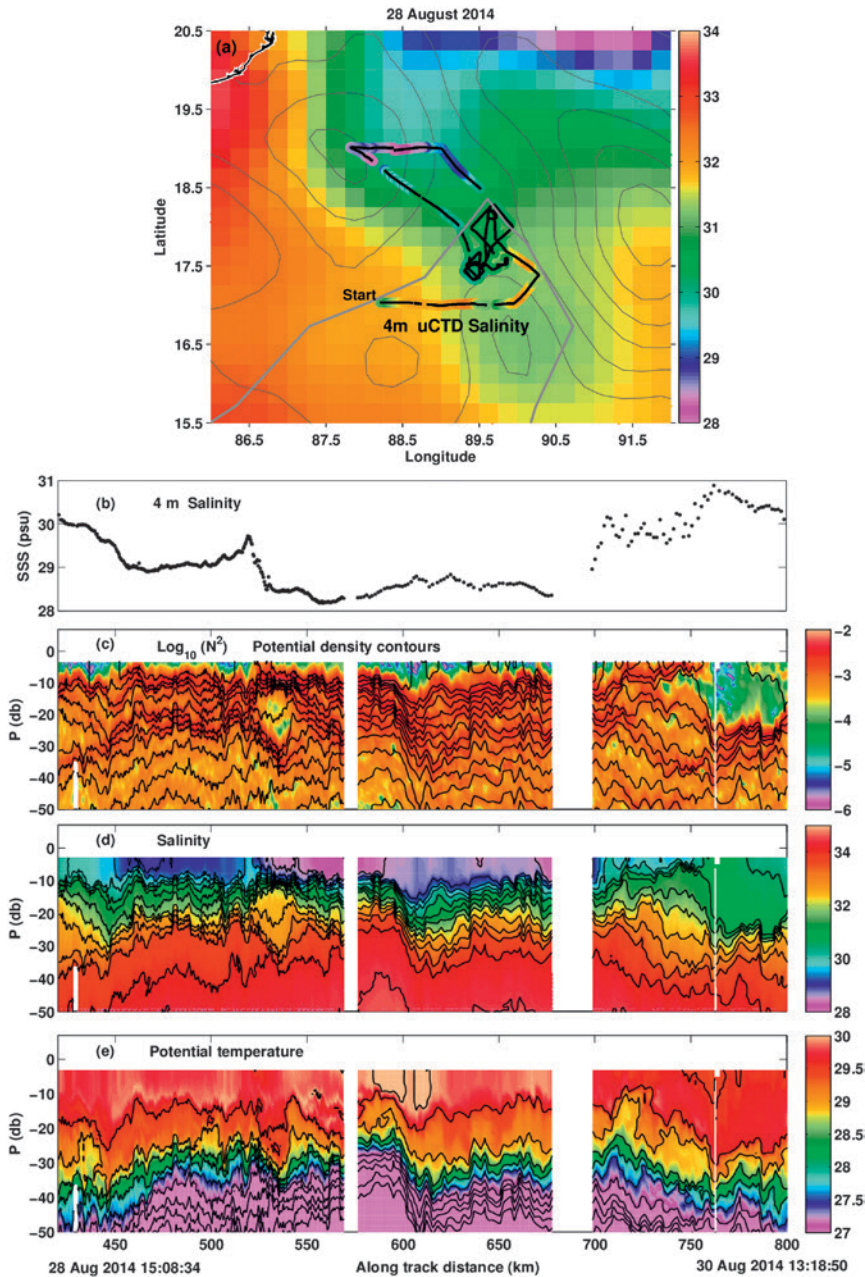
Fig. 10. (a) R/V *Sagar Nidhi* survey tracks on 28–30 Aug 2014 marked with 4-m salinity measured by an underway CTD system superimposed on an SSS map with SSHA contours on 28 Aug 2014: (b) 4-m salinity, (c) $\log_{10}$ values of squared Brunt–Väisälä frequency [$\log_{10}(N^2)$; color shading] in s^{-2} and potential density contours in kg m^{-3}, (d) salinity in psu, and (e) potential temperature in °C.

the surface density) ranged between 5 and 30 m, and the euphotic depths ranged between 60 and 104 m. The oxycline and nitracline follow closely with the 1,022 kg m^{-3} isopycnal. Chl-FL shows the presence of a deep chlorophyll maximum (DCM) that roughly tracked the 1,022 kg m^{-3} isopycnal (Fig. 11). The BoB is one of the major oxygen minimum zones of the world, where the suppression of convective overturning by freshwater stratification prevents ventilation of the pycnocline. Here, phytoplankton production within the pycnocline could be an important source of oxygen for heterotrophs in the upper pycnocline.

A comparison of *T–S* properties derived from Argo and the 2013 shipboard underway CTD data (spatial resolution of a few kilometers) highlights water masses and thermohaline gradients across the basin (Figs. 12, 13). The northern end of the BoB is considerably fresher than the south-central BoB (SSS near 30 psu as compared to 33 psu). During November–December 2013, the lowest-salinity water resides in the northeast corner of the BoB. The warm, high-salinity (>34 psu) Arabian Sea water can be found in the thermocline near 50–70 m and

casts during the cruise. Each cast provided a vertical profile of temperature, salinity, nitrate, dissolved oxygen (DO), chlorophyll fluorescence (Chl-FL), photosynthetically available radiation (PAR), and AOPs and IOPs up to a depth of 220 m (Fig. 11). Nitrate was measured with a Submersible Ultraviolet Nitrate Analyzer (SUNA V2) ultraviolet sensor. ML depths (estimated as the depth where density differs by 0.1 kg m^{-3} from

in a high-salinity layer near 120–150 m (Fig. 13). The Argo comparison allows inference of the likely origin of the waters within the observed eddy field, including an intrathermocline eddy (ITE; Fig. 14) and reconstruction of the regional circulation patterns. The geostrophic current relative to 200 m, marking the base of the ITE, showed a maximum current of ~0.25 m s^{-1} at 70–80-m depth. The surface current

was about 50% of the subsurface velocity maximum, so the ITE did have a surface expression in the velocity field, which is unlike the ITE observed in the Sea of Japan (Gordon et al. 2002).

Finescale fronts, filaments, and internal waves. Thermal fronts can play a significant role in air–sea interactions, upper-ocean vertical structure, biological productivity, lateral and vertical mixing processes, and modification of cyclone tracks, but these features have received scant attention (Ramachandran et al. 2014). Preliminary analysis shows that the high-resolution (1 km) GHRSST daily mean product allows for detection of sharp frontal features during cloud-free conditions (Fig. 15). The subsurface details of one example front are captured by the wirewalker array data (Fig. 16). In this example, three profilers were released in a cluster with an initial separation of 3 km, spanning a front, and allowed to drift for ~2 days while the ship traversed short sections with the underway CTD, pole-mounted ADCP, and bow chain. During the drift, the vertical structure above the main pycnocline was dominated by salinity stratification (Figs. 16c,d). The mixed layer deepened by >20 m over roughly 24 h and 5-km drift, coincident with a subsurface temperature maximum of decreasing thickness. Squared vertical shear in the horizontal currents was intensified at the base of the mixed layer and, at times, within the pycnocline (Fig. 16f). The turbulent heat flux based on observations of temperature–variance dissipation rate χ showed an upward heat flux across the base of the mixed layer of ~5–10 W m^{-2} associated with elevated dissipation and
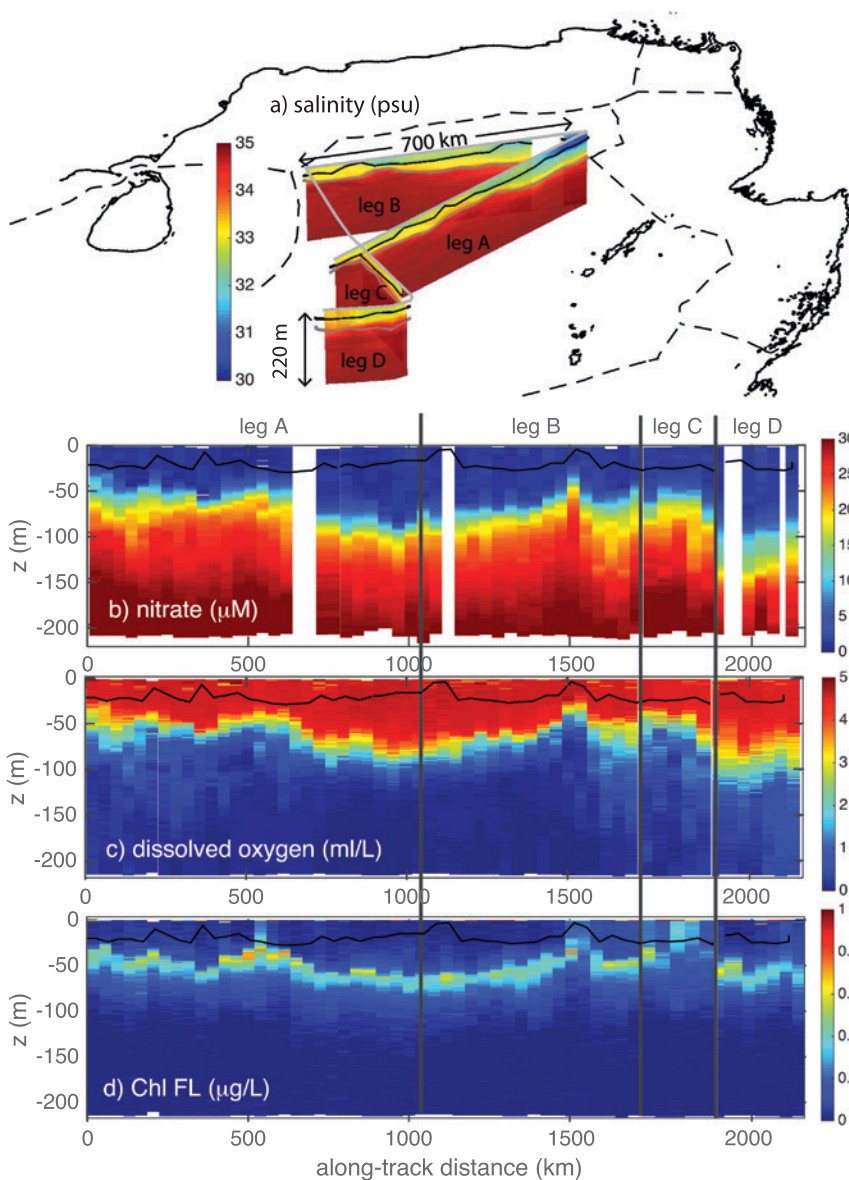

Fig. 11. (a) Map showing the boundaries of the Bay of Bengal and the country EEZs (dotted). The ship's track is denoted by the curtain plot, which shows salinity in the upper 220 m (blue is fresh and red is saline). Vertical Z along-track sections of (b) nitrate, (c) dissolved oxygen, and (d) chlorophyll fluorescence plotted along the ship's trajectory. These were measured on the CTD casts, several of which are missing in leg C because of the passage of a hurricane. Legs A, B, C, and D refer to the sections shown in (a), where A traverses northward, B traverses southward, C traverses eastward, and D traverses southward.

the local subsurface thermal maximum, including increased SST (Fig. 16g). Elevated chlorophyll, centered at ~30 m, was observed in association with the front (Fig. 16e). The measured chlorophyll fluorescence was significantly higher than that observed elsewhere. The pycnocline is characterized by interleaving of density-compensated temperature and salinity features with small vertical scales (<10 m) associated with elevated
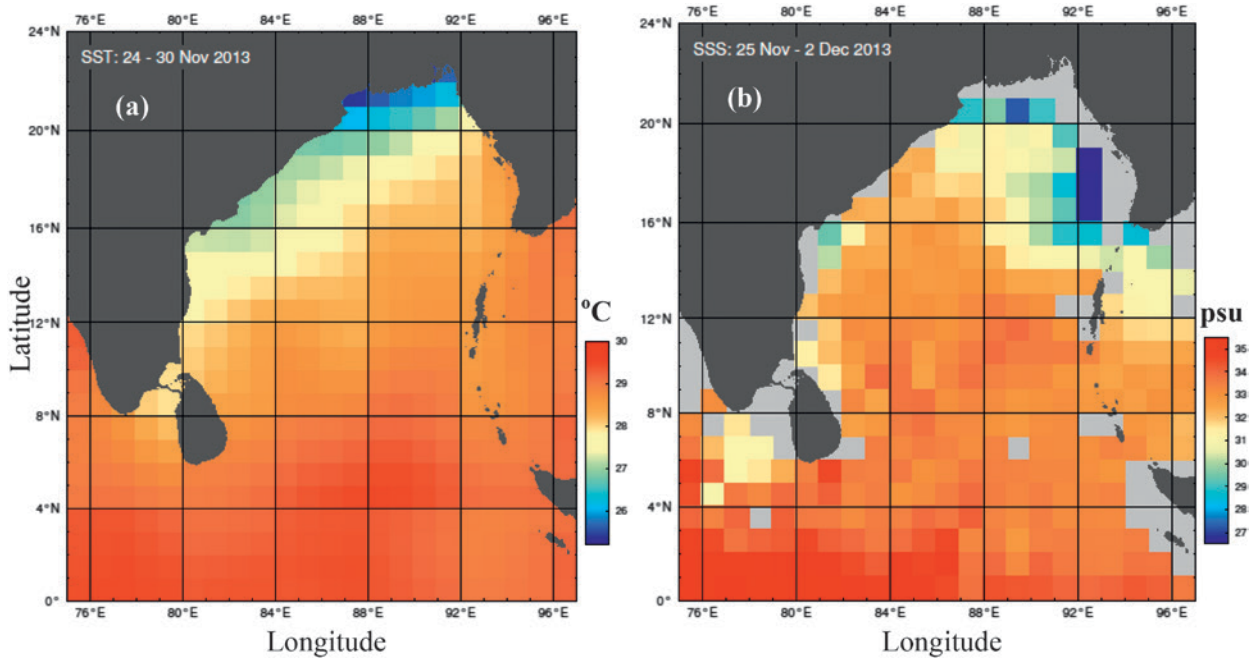
FIG. 12. (a) SST 24–30 Nov 2013 from Reynolds dataset (http://iridl.ldeo.columbia.edu/SOURCES/.NOAA /.NCEP/.EMC/.CMB/.GLOBAL/.Reyn_SmithOIv2/.weekly/.sst/). Relatively low SST with values below 27°C is observed along the northwestern Bay of Bengal margin and at the northern apex with values below 25°. (b) SSS from Aquarius V4 (http://podaac.jpl.nasa.gov/aquarius) for the period 25 Nov–2 Dec 2013. Low SSS arc along the land margins, with the lowest values, below 30, found in the northern and northeastern margin of the Bay of Bengal. The central axis of the Bay of Bengal displays SSS near 34. The gray areas do not have Aquarius SSS due to contamination from the land.

shear and χ (Figs. 16f,g). These features were especially notable below regions of elevated chlorophyll feature.

The internal wave climate of the BoB is poorly characterized, apart from relatively sparse measurements of the semidiurnal tides and high-frequency waves obtained over the past several decades (e.g., Wijeratne et al. 2010; Jackson 2007; Antony et al. 1985; Osborne and Burch 1980; Perry and Schimke 1965). ASIRI observations provide new insights into the internal wavefield through the NRL mooring array (Fig. 1), which spanned the path of tidal beams radiating from Andaman–Nicobar Island gaps toward Sri Lanka (e.g., Jackson 2007). Displacement spectra of internal waves at 6.5°N, 87°E were computed from moored temperature records (20-month-long records at 1-min resolution) following Levine et al. (1987). The displacement spectra show diurnal and semidiurnal (M2) tides, several superharmonics of tides, and high-frequency bump at approximately one-fifth of the local buoyancy frequency (Fig. 17). The energy levels at higher-frequency bands are significantly larger than the canonical open-ocean estimates specified in the Garrett–Munk spectral model (Garrett and Munk 1979), suggesting that tidally driven mixing may be a significant factor in the southern BoB.

Atmospheric boundary layer during non-MJO period. The beginning of ASIRI–RAWI campaign coincided with the decaying phase of the MJO signal over the tropics according to the Real-time Multivariate MJO index (Wheeler and Hendon 2004), thus permitting observations of subseasonal non-MJO phenomena. For example, both the Seychelles and Singapore observations contained high-speed (~5 m s^{-1}) packets of zonal winds (jets) with wavelengths on the order of ~10,000 km and at ~15-km heights propagating eastward, suggesting their similarity to equatorial Kelvin waves (Wallace and Kousky 1968; Andrews et al. 1987). Their influence propagated to the ground level through quasi-periodic biweekly breakdown of the lower boundary of the zonal jet, possibly by shear (Yamamoto et al. 2003), resulting in periodic ground level wind bursts.

Of particular interest to ASIRI (OMM and EBOB) was the Sri Lanka meteorological site located close to the BoB (Fig. 18a). The time series of meridional and zonal wind profiles are given in Figs. 18b and 18c. Although regular zonal wind oscillations observed at other sites were absent here, the zonal flow in Sri Lanka was also elevated at ~15 km (9 February). The downward descent of this westerly jet, again possibly
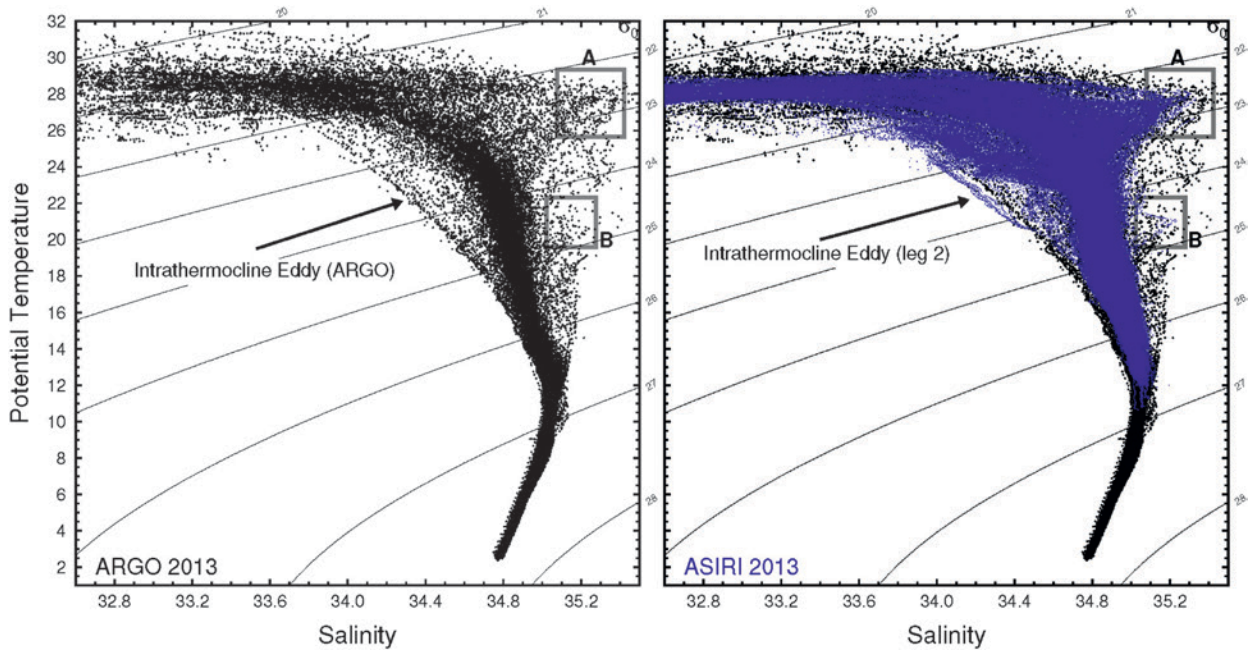
FIG. 13. Potential temperature (θ, °C) vs salinity (S) for the (left) 2013 Argo profiles within the Bay of Bengal and for the (right) ASIRI 2013 CTD station and underway data: blue dots are the ASIRI data, and black dots are the Argo (same as shown in the left). The low-salinity surface water overlies significant saltier thermocline water. Box A locates a distinct salinity maximum commonly found in the central Bay of Bengal within the 50- to 70-m depth interval drawn from the Arabian Sea. Box B denotes a salinity maximum in the 120–150-m depth interval that is occasionally observed. Box C is low-salinity, upper-thermocline water found within the northern mesoscale survey of ASIRI leg 1. The intrathermocline eddy observed during ASIRI cruise 2 (see Fig. SB2) falls on the low-salinity extreme of the thermocline θ–S scatter. The Argo profiles observe similar θ–S water in the eastern BoB.
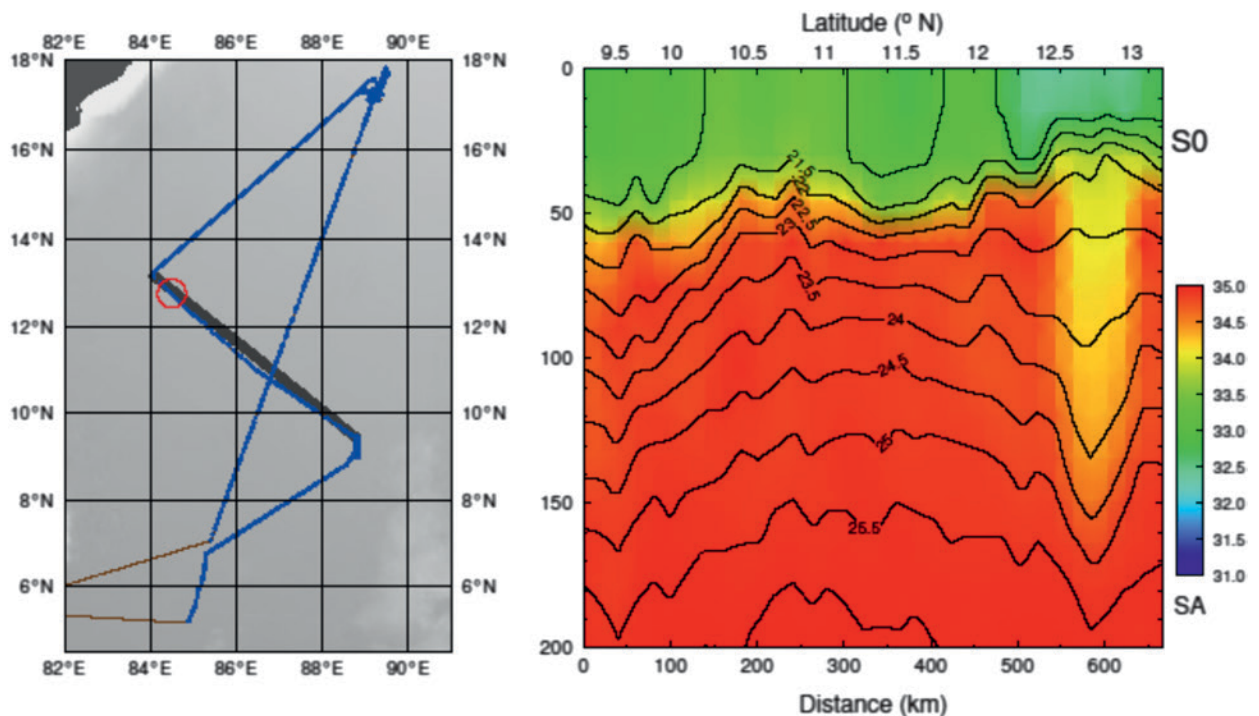

FIG. 14. (left) The R/V *Roger Revelle* leg-2 cruise track. The location of the ITE is marked by the red circle. (right) Salinity (color image) and overlaid isopycnal contours show the ITE.
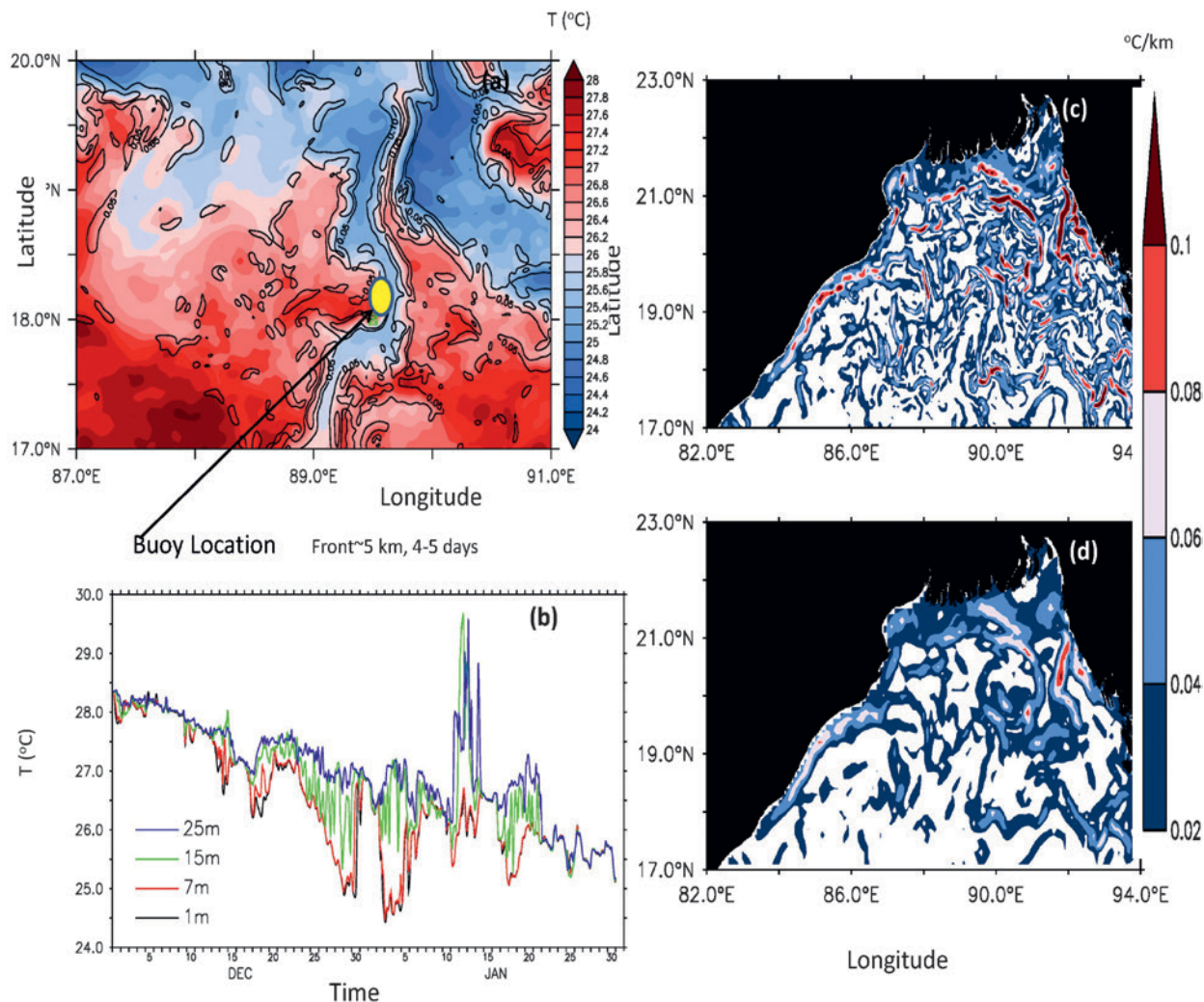
Fig. 15. (a) Thermal fronts can be seen in the northern BoB from a composite satellite SST image and **(b)** time series of near-surface temperature at four different depths from a buoy at 18°N, 89.5°E. Horizontal SST gradient magnitude (°C km⁻¹) for 15 Jan 2013. The estimated temperature gradients based on **(c)** 1-km resolution and **(d)** 10-km resolution.

initiated by shear at the lower boundary, occurred rapidly until ~5-km (on 11 February) height, prompted by weakly stable atmospheric conditions prone to shear instabilities (i.e., low gradient Richardson number Ri_g). A very stable layer centered around 4 km with maximum Ri_g ~ 10–15 (Fig. 18f) impeded the descent, though downward mixing may have continued across the stable layer at a slower rate. By 15 February, maximum Ri_g decreased to ~4, approaching Ri_g ~ 1 at the edges of the stable shear layer. Note that the low-resolution radiosonde measurements, in this case of resolution ~25 m, could overestimate the Ri_g, as shown by De Silva et al. (1999). The condition of $Ri_g \approx 1$ corresponds to the maximum rate of stratified turbulent mixing (Strang and Fernando 2001) and hence could transport significant amounts of dry air from aloft toward the surface. This air mixed with existing surface

moist air [70%–90% relative humidity (RH)], thus reducing the ground level RH, followed by a temperature drop due to evaporative cooling (cf. 15–17 February in Figs. 18d,e). Rain events (9, 10, 11, and 13 February), local urbanization, and advection of moist air by the near-surface northwesterly flow over the ocean appear to have contributed to the high RH prior to this event.

The drop of surface temperature impeded convective activity, as evident from the reduced heat flux and velocity variances (Fig. 18e) as well as the height of the capping inversion (ceilometer). Reduced moisture led to the suppression of rainfall until 25 February, whence the surface moisture has increased to the previous levels and the upper-level moisture has increased substantially to resuscitate rainfall activity. The same patterns for RH and temperature were recorded by the instrumented buoy at 8°N, 90°E
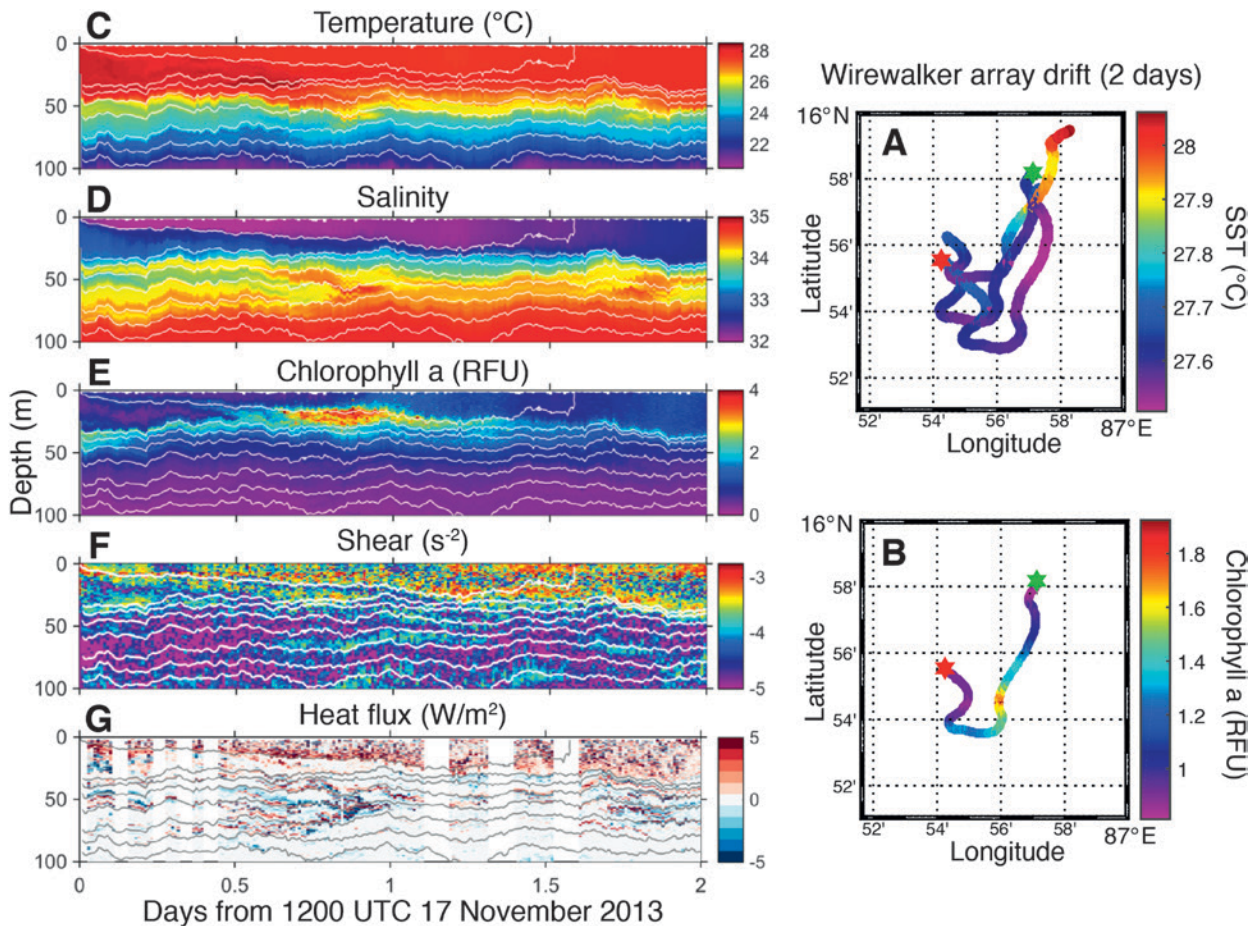
FIG. 16. A 2-day drift of two wirewalkers near 16°N and 87°E in Nov 2013. (a) SST along the drift from each wirewalker. (b) Mean chlorophyll in the upper 50 m. [The elevated chlorophyll at 15°55'N, 86°56'E is the subsurface feature in (e)]. Depth–time sections of (c) temperature, (d) salinity, (e) chlorophyll, (f) shear squared, and (g) turbulent heat flux. Overlaid thin lines are density contours. The green and red stars in (a) indicate the beginning and end of the drifts, respectively, of the wirewalker time series presented in (c)–(g).

in the BoB, within the same latitudinal band as the Sri Lanka site, which is a part of the RAMA program (McPhaden et al. 2009). This suggests that the vertical transport phenomena observed in Sri Lanka may also be occurring in the BoB, leading to the modulations of near-surface heat and moisture fluxes, thus affecting the air–sea exchange processes. These results point to the significant role that multiscale atmospheric processes, from regional-scale upper-atmospheric flows to entrainment across stratified layers to mixing in the ABL, play in air–sea interactions of the BoB.

SUMMARY AND CONCLUDING REMARKS. ASIRI, a 5-yr (2013–17) research effort of the United States, India, and Sri Lanka is aimed at understanding and quantifying coupled atmosphere–ocean dynamics relevant to the Indian Ocean monsoons. The program has already generated an unprecedented ocean and atmospheric dataset covering multiple space–time

processes and model simulations for the BoB. ASIRI has combined multiple observational assets, including multimonth shipboard surveys in three different years, long-term mooring, drifter, float, and glider deployments, and short-term deployments of a variety of autonomous assets (gliders, drifters, floats, and wirewalkers) in order to resolve upper-ocean structure, circulation, and air–sea interactions at spatial scales ranging from basinwide to the microscale.

Preliminary analyses have resolved the salinity and temperature gradients across BoB at resolution down to $O(1)$ km, offering high-resolution detail of submesoscale to mesoscale features. Mesoscale features of interest include the intrathermocline eddies and the seasonally forming cyclonic eddy, the "Sri Lanka dome," as previously reported by several investigators (e.g., Vinayachandran et al. 1999, 2013). The EICC and its northward-flowing offshore counterpart have been resolved at high resolution, and
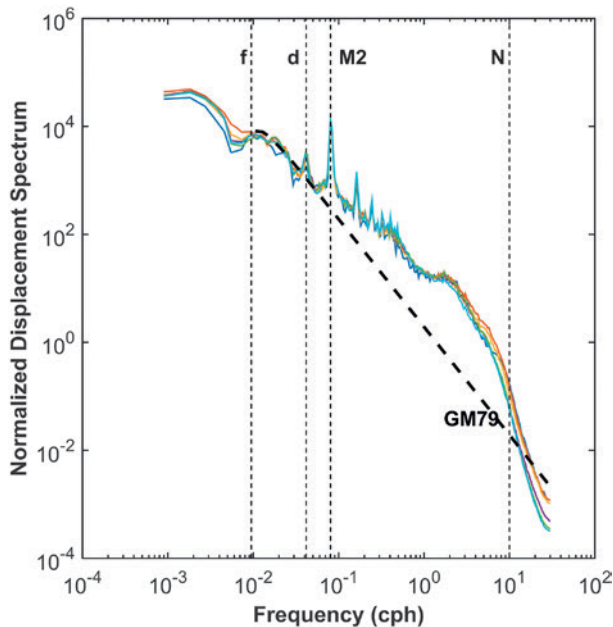
Fig. 17. Normalized displacement spectra at 6.5°N, 87°E. Six spectral estimates based on 20-month-long records at 80-, 90-, 95-, 105-, 110-, and 125-m depth levels are shown; *f, d*, M2, and *N* are inertial frequency, diurnal frequency, semidiurnal frequency, and local buoyancy frequency in cycles per hour (cph). The sampling rate of temperature was 60 cph. The displacement spectrum was normalized by multiplying by the local buoyancy frequency (e.g., Levine et al. 1987). GM79 denotes the Garrett–Munk spectral level corresponding to the local inertial frequency (Garrett and Munk 1979).

the combination of these observations with model simulations provides a means of better defining the contribution of such features to the BoB heat and salt balances. Numerical simulations have shown submesoscale signatures of the shallow, stratified layers in the BoB are markedly different than those of deep $O(100)$ m wintertime mixed layers, confirming earlier observational and numerical studies. Sharp frontal features are pronounced in the northern BoB, where shallow, salinity-controlled mixed layers result from high river runoff and heavy rainfall. Here, lateral stirring processes and vertical mixing near fronts may determine water mass modification. In the southern BoB, energetic internal waves, which were observed along an internal wave beam extending from the Andaman–Nicabor Island gaps, have potential energy levels one order of magnitude larger than those of the open ocean, suggesting that high-frequency internal waves may play an important role in mixing in some regions.

The ABL observations during the decaying phase of the MJO signal permitted observations of subseasonal, non-MJO phenomena, pointing to the significant role that multiscale atmospheric processes play in air–sea interactions in the BoB. An integrated analysis of satellite observations, numerical simulations, and in situ data has already begun and is expected to shed light on how regional-scale oceanic and atmospheric processes control the ABL and upper-ocean ML processes and their interactions, which in turn provide strong feedback on larger-scale processes, including monsoons and their breaks. Processes in the BoB have the potential to have strong effects on regional and global climate patterns, including modifying the atmospheric circulation, heat and salt exchange in the Indian Ocean, and altering of the monsoon and rain patterns.

Ongoing analyses of these atmospheric and oceanic datasets gathered in 2013–17 will allow a greater understanding of upper-ocean circulation and thermodynamics of the northern Indian Ocean and its coupling to the atmospheric circulation including monsoons.

MARINE MAMMAL OBSERVATIONS

A cetacean sighting survey was conducted by an international team of eight observers during the basinwide November 2013 cruise to characterize community composition and the distribution of cetaceans with respect to mesoscale oceanographic features. Cetacean sighting data were collected using binoculars and the naked eye, with the standard marine mammal survey methodology (e.g., Alling et al. 1991). A 1,669-km trackline was surveyed in Beaufort 5 or less sea conditions, and 52 sightings of 12 different species were recorded, including spinner dolphin, striped dolphin, false killer whale, pantropical spotted dolphin, bottlenose dolphin, Risso's dolphin, common dolphin, sperm whale, pygmy killer whale, pygmy/dwarf sperm whale, blue whale, and killer whale. Sightings were mostly concentrated in the southern BoB, with few cetaceans encountered in the central and northern bay. However, sighting conditions were better in the southern bay when compared to the central and northern bay, so it is unclear if the observed differences in sighting rates between the northern and southern BoB were real. Integrating additional sighting data with concurrent oceanographic observations in this region will help elucidate how cetacean occurrence and distribution are influenced by the monsoons.
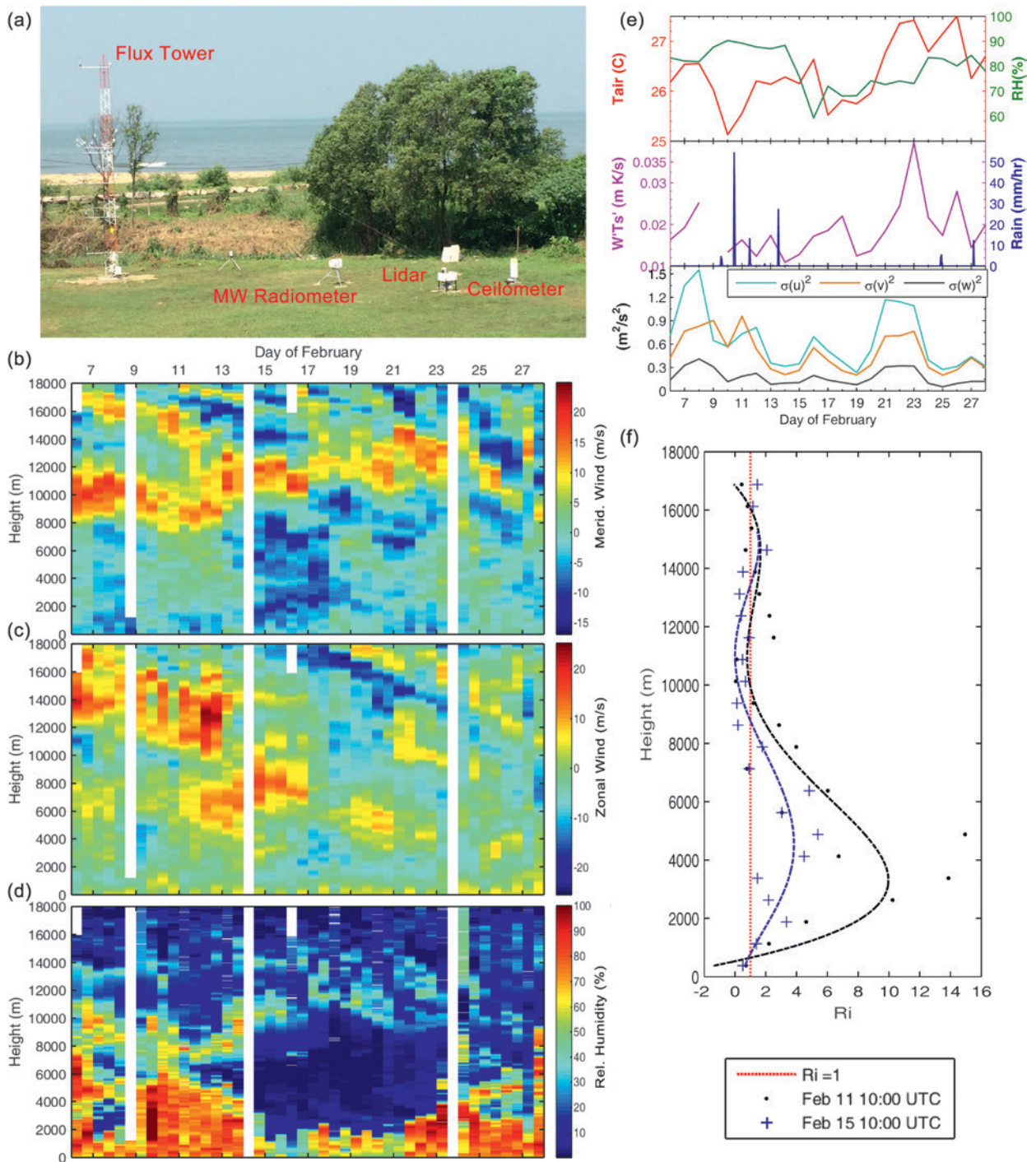
FIG. 18. (a) Measurement site in Colombo, Sri Lanka; height–time plots of (b) meridional wind, (c) zonal wind, and (d) relative humidity from the sounding station at the Sri Lanka site. (e) Daily averaged values of RH, air temperature (Tair), rainfall rate (Rain), and streamwise, crosswise, and vertical velocity variances $\sigma^2(u)$, $\sigma^2(v)$, $\sigma^2(w)$ measured at the flux tower in Sri Lanka. (f) Vertical profiles of bin-averaged gradient Richardson number in two different representative soundings.

REFERENCES

Allard, R. A., and Coauthors, 2012: Validation test report for the Coupled Ocean/Atmosphere Mesoscale Prediction System (COAMPS) version 5.0: Ocean/wave component validation. Naval Research Laboratory Rep. NRL/MR/7320–12-9423, 101 pp. [Available online at www.dtic.mil/dtic/tr/fulltext/u2/a577284.pdf.]

Alling, A. K., E. M. Dorsey, and J. C. D. Gordon, 1991: Blue whales (*Balaenoptera musculus*) off the northeast coast of Sri Lanka: Distribution, feeding and individual identification. Cetaceans and Cetacean Research in the Indian Ocean Sanctuary, UNEP Marine Mammal Technical Rep. 3, 247–258.

Andrews, D. G., J. R. Holton, and C. B. Leovy, 1987: *Middle Atmosphere Dynamics.* Academic Press, 489 pp.

Antony, M. K., C. S. Murty, G. V. Reddy, and K. H. Rao, 1985: Sub-surface temperature oscillations and associated flow in the western Bay of Bengal. *Estuarine Coastal Shelf Sci.*, **21**, 823–834, doi:10.1016/0272-7714(85)90076-9.

Arobone, E., and S. Sarkar, 2015: Effects of three-dimensionality on instability and turbulence in a frontal zone. *J. Fluid Mech.*, **784**, 252–273, doi:10.1017/jfm.2015.564.

Bhat, G. S., and Coauthors, 2001: BOBMEX: The Bay of Bengal Monsoon Experiment. *Bull. Amer. Meteor. Soc.*, **82**, 2217–2243, doi:10.1175/1520-0477(2001)082<2217:BTBOBM>2.3.CO;2.

Boccaletti, G., R. Ferrari, and B. Fox-Kemper, 2007: Mixed layer instabilities and restratification. *J. Phys. Oceanogr.*, **37**, 2228–2250, doi:10.1175/JPO3101.1.

Booij, N., R. C. Ris, and L. H. Holthuijsen, 1999: A third-generation wave model for coastal regions. Part I: Model description and validation. *J. Geophys. Res.*, **104**, 7649–7666, doi:10.1029/98JC02622.

Chen, S., and Coauthors, 2003: COAMPS version 3 model description general theory and equations. Naval Research Laboratory Rep. NRL/PU/7500-03-448, 143 pp.

——, and Coauthors, 2015: A study of CINDY/DYNAMO MJO suppressed phase. *J. Atmos. Sci.*, **72**, 3755–3779, doi:10.1175/JAS-D-13-0348.1.

Cheng, X., S. P. Xie, J. P. McCreary, Y. Qi, and Y. Du, 2013: Intraseasonal variability of sea surface height in the Bay of Bengal. *J. Geophys. Res. Oceans*, **118**, 816–830, doi:10.1002/jgrc.20075.

D'Asaro, E., C. Lee, L. Rainville, L. Thomas, and R. Harcourt, 2011: Enhanced turbulence and energy dissipation at ocean fronts. *Science*, **332**, 318–322, doi:10.1126/science.1201515.

De Silva, I. P. D., A. Brandt, L. J. Montenegro, and H. J. Fernando, 1999: Gradient Richardson number measurements in a stratified shear layer. *Dyn. Atmos. Oceans*, **30**, 47–63, doi:10.1016/S0377-0265(99)00015-9.

Durand, F., D. Shankar, F. Birol, and S. S. C. Shenoi, 2009: Spatiotemporal structure of the East India Coastal Current from satellite altimetry. *J. Geophys. Res.*, **114**, C02013, doi:10.1029/2008JC004807.

Fox-Kemper, B., R. Ferrari, and B. Hallberg, 2008: Parameterization of mixed layer eddies. Part I: Theory and diagnosis. *J. Phys. Oceanogr.*, **38**, 1145–1165, doi:10.1175/2007JPO3792.1.

Gadgil, S., 2003: The Indian monsoon and its variability. *Annu. Rev. Earth Planet. Sci.*, **31**, 429–467, doi:10.1146/annurev.earth.31.100901.141251.

Garrett, C., and W. Munk, 1979: Internal waves in the ocean. *Annu. Rev. Fluid Mech.*, **11**, 339–369, doi:10.1146/annurev.fl.11.010179.002011.

Girishkumar, M. S., M. Ravichandran, and M. J. McPhaden, 2013: Temperature inversions and their influence on the mixed layer heat budget during the winters of 2006–2007 and 2007–2008 in the Bay of Bengal. *J. Geophys. Res. Oceans*, **118**, 2426–2437, doi:10.1002/jgrc.20192.

Gordon, A. L., C. F. Giulivi, C. L. Lee, H. H. Furey, A. Bower, and L. Talley, 2002: Japan/East Sea intrathermocline eddies. *J. Phys. Oceanogr.*, **32**, 1960–1974, doi:10.1175/1520-0485(2002)032<1960:JESIE>2.0.CO;2.

Hodur, R. M., 1997: The Naval Research Laboratory's Coupled Ocean/Atmosphere Mesoscale Prediction System (COAMPS). *Mon. Wea. Rev.*, **125**, 1414–1430, doi:10.1175/1520-0493(1997)125<1414:TNRLSC>2.0.CO;2.

Jackson, C. R., 2007: Internal wave detection using the Moderate Resolution Imaging Spectroradiometer (MODIS). *J. Geophys. Res.*, **112**, C11012, doi:10.1029/2007JC004220.

Jensen, T. G., 2001: Arabian Sea and Bay of Bengal exchange of salt and tracers in an ocean model. *Geophys. Res. Lett.*, **28**, 3967–3970, doi:10.1029/2001GL013422.

——, 2003: Cross-equatorial pathways of salt and tracers from the north Indian Ocean: Modelling results. *Deep-Sea Res. II*, **50**, 2111–2127, doi:10.1016/S0967-0645(03)00048-1.

——, T. Shinoda, S. Chen, and M. Flatau, 2015: Ocean response to CINDY/DYNAMO MJOs in air-sea-coupled COAMPS. *J. Meteor. Soc. Japan*, **93A**, 157–178, doi:10.2151/jmsj.2015-049.

Kurien, P., M. Ikeda, and V. K. Valsala, 2010: Mesoscale variability along the east coast of India in spring as revealed from satellite data and OGCM simulations. *J. Oceanogr.*, **66**, 273–289, doi:10.1007/s10872-010-0024-x.

Lagerloef, G., R. Schmitt, J. Schanze, and H. Y. Kao, 2010: The ocean and the global water cycle. *Oceanography*, **23**, 82–93, doi:10.5670/oceanog.2010.07.

Levine, M. D., C. A. Paulson, and J. H. Morison, 1987: Observations of internal gravity waves under the Arctic pack ice. *J. Geophys. Res.*, **92**, 779–782, doi:10.1029/JC092iC01p00779.

Lucas, A. J., and Coauthors, 2014: Mixing to monsoons: Air-sea interactions in the Bay of Bengal. *Eos, Trans. Amer. Geophys. Union*, **95**, 269–270, doi:10.1002/2014EO300001.

Madden, R., and P. Julian, 1971: Detection of a 40–50 day oscillation in the zonal wind in the tropical Pacific. *J. Atmos. Sci.*, **28**, 702–708, doi:10.1175/1520-0469(1971)028<0702:DOADOI>2.0.CO;2.

Mahadevan, A., and A. Tandon, 2006: An analysis of mechanisms for submesoscale vertical motion at ocean fronts. *Ocean Modell.*, **14**, 241–256, doi:10.1016/j.ocemod.2006.05.006.

——, E. D'Asaro, C. Lee, and M. J. Perry, 2012: Eddy-driven stratification initiates North Atlantic spring phytoplankton blooms. *Science*, **337**, 54–58, doi:10.1126/science.1218740.

Martin, P. J., 2000: Description of the Navy Coastal Ocean Model version 1.0. Naval Research Laboratory Rep. NRL/FR/7322/00/9962, 45 pp. [Available from Naval Research Laboratory, Code 7322, Bldg. 1009, Stennis Space Center, MS 39529-5004.]

McCreary, J. P., W. Han, D. Shankar, and S. R. Shetye, 1996: Dynamics of the East India Coastal Current: 2. Numerical solutions. *J. Geophys. Res.*, **101**, 13 993–14 010, doi:10.1029/96JC00560.

McPhaden, M. J., and Coauthors, 2009: RAMA: The Research Moored Array for African–Asian–Australian Monsoon Analysis and Prediction. *Bull. Amer. Meteor. Soc.*, **90**, 459–480, doi:10.1175/2008BAMS2608.1.

Moum, J. N., and J. D. Nash, 2009: Mixing measurements on an equatorial ocean mooring. *J. Atmos. Oceanic Technol.*, **26**, 317–336, doi:10.1175/2008JTECHO617.1.

Mukherjee, A., and Coauthors, 2014: Observed seasonal and intraseasonal variability of the East India Coastal Current on the continental slope. *J. Earth Syst. Sci.*, **123**, 1197–1232, doi:10.1007/s12040-014-0471-7.

Murty, V. S. N., Y. V. B. Sarma, D. P. Rao, and C. S. Murty, 1992: Water characteristics, mixing and circulation in the Bay of Bengal during southwest monsoon. *J. Mar. Res.*, **50**, 207–228, doi:10.1357/002224092784797700.

——, ——, and ——, 1996: Variability of the oceanic boundary layer characteristics in the northern Bay of Bengal during MONTBLEX-90. *Proc. Indian Acad. Sci.*, **105**, 41–61. [Available online at http://drs.nio.org/drs/handle/2264/2261.]

Niiler, P. P., 2001: The World Ocean surface circulation. *Ocean Circulation and Climate: Observing and Modelling the Global Ocean*, G. Siedler, J. Church, and J. Gould, Eds., Academic Press, 193–204.

Osborne, A. R., and T. L. Burch, 1980: Internal solitons in the Andaman Sea. *Science*, **208**, 451–460, doi:10.1126/science.208.4443.451.

Perry, R. B., and G. R. Schimke, 1965: Large-amplitude internal waves observed off the northwest coast of Sumatra. *J. Geophys. Res.*, **70**, 2319–2324, doi:10.1029/JZ070i010p02319.

Pham, H. T., S. Sarkar, and K. B. Winters, 2013: Large-eddy simulation of deep-cycle turbulence in an Equatorial Undercurrent model. *J. Phys. Oceanogr.*, **43**, 2490–2502, doi:10.1175/JPO-D-13-016.1.

Pinkel, R., M. A. Goldin, J. A. Smith, O. M. Sun, A. A. Aja, M. N. Bui, and T. Hughen, 2011: The wirewalker: A vertically profiling instrument carrier powered by ocean waves. *J. Atmos. Oceanic Technol.*, **28**, 426–435, doi:10.1175/2010JTECHO805.1.

Potemra, J. T., M. E. Luther, and J. J. O'Brien, 1991: The seasonal circulation of the upper ocean in the Bay of Bengal. *J. Geophys. Res.*, **96**, 12 667–12 683, doi:10.1029/91JC01045.

Rainville, L., and R. Pinkel, 2001: Wirewalker: An autonomous wave-powered vertical profiler. *J. Atmos. Oceanic Technol.*, **18**, 1048–1051, doi:10.1175/1520-0426(2001)018<1048:WAAWPV>2.0.CO;2.

Ramachandran, S., A. Tandon, and A. Mahadevan, 2014: Enhancement in vertical fluxes at a front by mesoscale-submesoscale coupling. *J. Geophys. Res. Oceans*, **119**, 8495–8511, doi:10.1002/2014JC010211.

Rao, R. R., and R. Sivakumar, 2003: Seasonal variability of sea surface salinity and salt budget of the mixed layer of the north Indian ocean. *J. Geophys. Res.*, **108**, 3009, doi:10.1029/2001JC000907.

Rao, S. A., and Coauthors, 2011: Modulation of SST, SSS over northern Bay of Bengal on ISO time scale. *J. Geophys. Res.*, **116**, C09026, doi:10.1029/2010JC006804.

Schott, F., and J. P. McCreary, 2001: The monsoon circulation of the Indian Ocean. *Prog. Oceanogr.*, **51**, 1–123, doi:10.1016/S0079-6611(01)00083-0.

——, J. Reppin, and J. Fisher, 1994: Currents and transports of the Monsoon Current south of Sri Lanka. *J. Geophys. Res.*, **99**, 25 127–25 141, doi:10.1029/94JC02216.

Sengupta, D., B. N. Goswami, and R. Senan, 2001: Coherent intraseasonal oscillations of ocean and atmosphere during the Asian summer monsoon. *Geophys. Res. Lett.*, **28**, 4127–4130, doi:10.1029/2001GL013587.

Shankar, D., P. N. Vinayachandran, and A. S. Unnikrishnan, 2002: The monsoon currents in the north Indian Ocean. *Prog. Oceanogr.*, **52**, 63–120, doi:10.1016/S0079-6611(02)00024-1.

Shenoi, S. S. C., D. Shankar, and S. R. Shetye, 2002: Differences in heat budgets of the near-surface Arabian Sea and Bay of Bengal: Implications for the summer monsoon. *J. Geophys. Res.*, **107**, 3052, doi:10.1029/2000JC000679.

Shetye, S. R., A. D. Gouveia, D. Shankar, S. S. C. Shenot, P. N. Vinayachandran, D. Sundar, G. S. Michael, and G. Nampoothiri, 1996: Hydrography and circulation in the western Bay of Bengal during the northeast monsoon. *J. Geophys. Res.*, **101**, 14 011–14 025, doi:10.1029/95JC03307.

Strang, E. J., and H. J. S. Fernando, 2001: Entrainment and mixing in stratified shear flows. *J. Fluid Mech.*, **428**, 349–386, doi:10.1017/S0022112000002706.

Vialard, J., S. S. C. Shenoi, J. P. McCreary, D. Shankar, F. Durand, V. Fernando, and S. R. Shetye, 2009: Intraseasonal response of the northern Indian Ocean coastal waveguide to the Madden–Julian oscillation. *Geophys. Res. Lett.*, **36**, L14606, doi:10.1029/2009GL038450.

Vinayachandran, P. N., Y. Masurnoto, T. Mikawa, and T. Yarnagata, 1999: Intrusion of the Southwest Monsoon Current into the Bay of Bengal. *J. Geophys. Res.*, **104**, 11 077–11 085, doi:10.1029/1999JC900035.

——, V. S. N. Murty, and V. Ramesh Babu, 2002: Observations of barrier layer formation in the Bay of Bengal during summer monsoon. *J. Geophys. Res.*, **107**, 8018, doi:10.1029/2001JC000831.

——, D. Shankar, S. Vernekar, K. K. Sandeep, P. Amol, C. P. Neema, and A. Chatterjee, 2013: A summer monsoon pump to keep the Bay of Bengal salty.

Geophys. Res. Lett., **40**, 1777–1782, doi:10.1002/grl.50274.

Wallace, J. M., and V. E. Kousky, 1968: Observational evidence of Kelvin waves in the tropical stratosphere. *J. Atmos. Sci.*, **25**, 900–907, doi:10.1175/1520-0469(1968)025<0900:OEOKWI>2.0.CO;2.

Webster, P. J., and Coauthors, 2002: The JASMINE pilot study. *Bull. Amer. Meteor. Soc.*, **83**, 1603–1630, doi:10.1175/BAMS-83-11-1603.

Wheeler, M. C., and H. H. Hendon, 2004: An all-season real-time multivariate MJO index: Development of an index for monitoring and prediction. *Mon. Wea. Rev.*, **132**, 1917–1932, doi:10.1175/1520-0493(2004)132<1917:AARMMI>2.0.CO;2.

Wijeratne, E. M. S., P. L. Woodworth, and D. T. Pugh, 2010: Meteorological and internal wave forcing of seiches along the Sri Lanka coast. *J. Geophys. Res.*, **115**, C03014, doi:10.1029/2009JC005673.

Wijesekera, H. W., and Coauthors, 2015: Southern Bay of Bengal currents and salinity intrusions during the northeast monsoon. *J. Geophys. Res. Oceans*, **120**, 6897–6913, doi:10.1002/2015JC010744.

Yamamoto, M. K., M. Fujiwara, T. Horinouchi, H. Hashiguchi, and S. Fukao, 2003: Kelvin-Helmholtz instability around the tropical tropopause observed with the equatorial atmosphere radar. *Geophys. Res. Lett.*, **30**, 1476, doi:10.1029/2002GL016685.

Yu, L., and M. J. McPhaden, 2011: Ocean preconditioning of Cyclone Nargis in the Bay of Bengal: Interaction between Rossby waves, surface fresh waters, and sea surface temperatures. *J. Phys. Oceanogr.*, **41**, 1741–1755, doi:10.1175/2011JPO4437.1.

——, J. J. O'Brien, and J. Yang, 1991: On the remote forcing of the circulation in the Bay of Bengal. *J. Geophys. Res.*, **96**, 20 449–20 454, doi:10.1029/91JC02424.